Reset PID Design for Motion Systems With Stribeck Friction

Ruud Beerens[ID], Andrea Bisoffi[ID], *Member, IEEE*, Luca Zaccarian[ID], *Fellow, IEEE*,
Henk Nijmeijer[ID], *Life Fellow, IEEE*, Maurice Heemels[ID], *Fellow, IEEE*,
and Nathan van de Wouw[ID], *Fellow, IEEE*

Abstract—**We present a reset control approach to achieve setpoint regulation of a motion system with a proportional-integral-derivative (PID)-based controller, subject to Coulomb friction and a velocity-weakening (Stribeck) contribution. While classical PID control results in persistent oscillations (hunting), the proposed reset mechanism induces asymptotic stability of the setpoint and significant overshoot reduction. Moreover, robustness to an unknown static friction level and an unknown Stribeck contribution is guaranteed. The closed-loop dynamics are formulated in a hybrid systems framework, using a novel hybrid description of the static friction element, and the asymptotic stability of the setpoint is proven accordingly. The working principle of the controller is demonstrated experimentally on a motion stage of an electron microscope, showing superior performance over classical PID control.**

Index Terms—**Friction, hybrid control, Lyapunov methods, motion control, stability analysis.**

I. INTRODUCTION

FRICTION is a performance-limiting factor in many high-precision motion systems for which many control techniques exist in the literature. A branch of control solutions relies on developing as-accurate-as-possible friction models, used for online compensation in a control loop [7], [24], [30], [31]. These model-based friction compensation methods are typically prone to model mismatches due to, e.g., unreliable friction measurements or time-varying or

uncertain friction characteristics. Model-based techniques, therefore, may suffer from overcompensation or undercompensation of friction, thereby resulting in loss of stability of the setpoint [38] and, thus, limiting the achievable positioning accuracy. Adaptive control methods [5], [19] provide some robustness to time-varying friction characteristics, but model mismatches (and the associated performance limitations) still remain. Nonmodel-based control schemes have also been proposed, examples of which are impulsive control [35], [46], dithering-based techniques [29], sliding-mode control [10], or switched control [34]. Apart from properly smoothed and parameterized sliding-mode control solutions [3], these nonmodel-based controllers may employ high-frequency control signals, risking excitation of high-frequency dynamics, in addition to raising tuning challenges. State feedback control techniques have been explored in [22] but do not provide a solution for the setpoint regulation control problem considered in this article.

Despite the availability of a wide range of (nonlinear) control techniques for frictional systems, linear controllers are still used in the vast majority of industrial motion systems due to the existence of intuitive design and tuning tools. In industry, the classical proportional-integral-derivative (PID) controller is commonly used for motion systems with friction. In particular, integral action ensures that the only possible equilibrium states correspond to zero position error (using the internal model property); therefore, *stability implies exact setpoint regulation.* Unfortunately, when the friction includes a velocity-weakening (i.e., Stribeck) effect [44], stability is generally lost, and steady-state oscillations emerge so that the internal model property cannot be applied. Intuitively speaking, as the integrator action builds up for compensating the static part of the friction, the velocity-weakening effect causes friction overcompensation as the velocity increases. As a result, the system overshoots the setpoint and ends up in persistent stick-slip oscillations (called *hunting*), as characterized in the modeling and analysis results of [7] and [27]. A much simpler scenario emerges in the Coulomb case (i.e., no Stribeck effect), wherein we recently proved [15] global asymptotic stability of the compact set of all the equilibria, despite the presence of Coulomb friction, for any possible linearly stabilizing PID gains tuning (preliminary results had been previously proven in [6]). For the simplified Coulomb case, we also recognized in [15, Remark 3] that the time-consuming process of filling the integrator buffer to overcome the static friction results in long settling times,

which motivated our recent reset integrator scheme [11] aimed at providing shorter settling times, thereby improving the transient performance, for the Coulomb case.

In this article, we provide a significant advancement compared to our former Coulomb-only (no Stribeck) scenarios of [11] and [15]. In particular, we propose a reset integral controller that achieves asymptotic stability of the setpoint, despite the presence of *unknown* static friction and an *unknown* velocity-weakening (Stribeck) effect in the friction characteristic. The proposed robust reset PID scheme is *model-free* (not model-based) and can be used as an augmentation of any linearly stabilizing PID controller.

Reset and hybrid controllers have been an active field of research in the past decades. Their development started with the Clegg integrator [21] and the first-order reset element [28]. Since then, reset controllers have mainly been used to improve the performance of *linear* motion systems [1], [32]. Specific examples are the hybrid integrator-gain system [23], [47], improving tracking performance and limiting overshoot. Overshoot reduction of linear systems using hybrid control is also presented, e.g., in [13] and [50]. Analysis and design tools for reset controllers are presented in [33] and [49] and in the recent overviews [9], [37]. Reset controllers have already been applied to improve *performance* of motion systems (notably, in our recent work [11] commented above) but have not been applied before for the *stabilization* of nonlinear frictional motion systems.

The contributions of this article are as follows. The first one is the design of a novel reset controller for systems with Stribeck friction, aiming at asymptotically stabilizing a constant setpoint. The second contribution is the development of a hybrid formulation of the closed-loop system, where the discontinuous friction element is captured by a hybrid simulation model (in the sense of [48, Definition 2.5]), instead of the commonly used set-valued force law [2, Sec. 1.3]. The simulation model builds upon our preliminary conference contribution in [14], where we now include the Stribeck effect and a radically different two-phase resetting law. The third contribution is proof of asymptotic stability, and the fourth contribution is an experimental demonstration of the effectiveness of the proposed controller on an industrial high-precision positioning system.

This article is organized as follows. In Section II, we present our reset PID controller design. In Section III, we formulate the reset closed loop as a hybrid system, state the main stability result, and exploit intrinsic robustness properties to obtain a suitable experimental implementation. In Section IV, we experimentally validate the proposed reset controller on a high-accuracy industrial positioning system. In Sections V and VI, we prove our main theorem establishing a number of useful intermediate results. The proofs of some technical lemmas are omitted due to space constraints but can be found [12], which is the publicly archived extended version of this article.

Notations: Given $x \in \mathbb{R}^n$, $|x|$ is its Euclidean norm. $\mathbb{B}$ is the closed unit ball, of appropriate dimensions, in the Euclidean norm. $\text{sign}(\cdot)$ denotes the classical sign function, i.e., $\text{sign}(y) := y/|y|$ for $y \neq 0$ and $\text{sign}(0) := 0$. $\text{Sign}(\cdot)$ (with an upper case S) denotes the *set-valued* sign function, i.e., $\text{Sign}(y) := \{\text{sign}(y)\}$ for $y \neq 0$, and $\text{Sign}(y) := [-1, 1]$ for $y = 0$. For $c > 0$, the deadzone function $y \mapsto dz_c(y)$ is defined as $dz_c(y) := 0$ if $|y| \leq c$; $dz_c(y) := y - c \, \text{sign}(y)$ if $|y| > c$. For column vectors $x_1 \in \mathbb{R}^{d_1}, \ldots, x_m \in \mathbb{R}^{d_m}$, the notation $(x_1, \ldots, x_m)$ is equivalent to $\begin{bmatrix} x_1^\top \cdots x_m^\top \end{bmatrix}^\top$. $e_3 := (0, 0, 1)$ is the third unit vector generating $\mathbb{R}^3$. $\wedge$, $\vee$, and $\implies$ denote the logical conjunction, disjunction, and implication.

For a hybrid solution ψ [25, Definition 2.6] with hybrid time domain dom ψ [25, Definition 2.3], the function $j(\cdot)$ is defined as $j(t) := \min_{(t,k) \in \text{dom } \psi} k$. Function $j(\cdot)$ depends on the specific solution ψ that it addresses, but, with a slight abuse of notation, we use a unified symbol $j(\cdot)$ because the solution under consideration is always clear from the context. A hybrid solution is maximal if it cannot be extended [25, Definition 2.7] and is complete if its domain is unbounded (in the t- or j-direction) [25, p. 30]. For a hybrid system $\mathcal{H}$ and a set S, $\psi \in \mathcal{S}_{\mathcal{H}}(x)$ (respectively, $\psi \in \mathcal{S}_{\mathcal{H}}(S)$) means that ψ is a maximal solution to $\mathcal{H}$ with $\psi(0, 0) = x$ (respectively, $\psi(0, 0) \in S$), and $\mathcal{S}_{\mathcal{H}}$ is the set of all maximal solutions to $\mathcal{H}$.

II. SYSTEM DESCRIPTION AND CONTROLLER DESIGN

A single-degree-of-freedom mass m sliding on a horizontal plane with position z_1 and velocity z_2 is subject to a control input $\bar{u}$ and a friction force belonging to a set $\Psi(z_2)$

$$\dot{z}_1 = z_2, \quad \dot{z}_2 \in \frac{1}{m}(\Psi(z_2) + \bar{u}). \tag{1}$$

The friction characteristic is modeled by the next set-valued (indicated by the double arrow) mapping of the velocity

$$z_2 \rightrightarrows \Psi(z_2) := -\bar{F}_s \, \text{Sign}(z_2) - \alpha z_2 + \bar{f}(z_2) \tag{2}$$

where $\bar{F}_s$ is the static friction, αz_2 the viscous friction contribution (with $\alpha \geq 0$ being the viscous friction coefficient), and $\bar{f}$ a nonlinear velocity-dependent friction contribution, encompassing the Stribeck effect. Recall that "Sign" denotes the set-valued sign function.

For a reference position $r \in \mathbb{R}$, our goal is formulated next.

Problem 1: Design a *reset* PID controller for $\bar{u}$ in (1) and (2) that globally asymptotically stabilizes the setpoint $(z_1, z_2) = (r, 0)$ without using knowledge of the friction parameters $\bar{F}_s$ and α and of function $\bar{f}$.

The advantage of using integrator action in Problem 1 is motivated by: 1) the fact that integral action is commonly used in the industry and that simple gain tuning rules are known to practitioners, thereby bridging the gap between control systems theory and control systems technology and 2) the fact that the integral action ensures that any equilibrium necessarily corresponds to zero steady-state position error, despite the *unknown* friction force. The need for reset mechanisms is motivated by the fact that stability of the setpoint is not achieved by *classical* PID feedback [15], [38]. Enhancing the PID controller with resets instead results in asymptotic stability of the setpoint, as shown in this article.
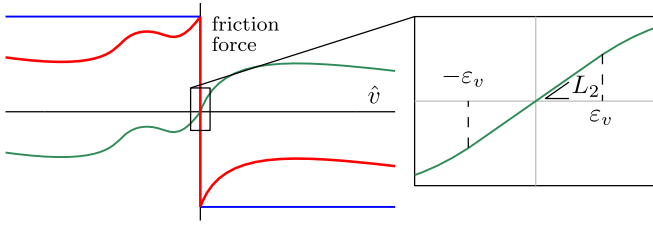
Fig. 1. Example of a friction force satisfying Assumption 1. Total friction (—), static contribution F_s (—), and velocity-dependent contribution f (—).

A. Classical PID Controller

Consider a *classical* PID controller for input $\bar{u}$ in (1), that is,

$$\bar{u} = -\bar{k}_p(z_1 - r) - \bar{k}_d z_2 - \bar{k}_i z_3, \quad \dot{z}_3 = z_1 - r \quad (3)$$

where z_3 is the PID controller state, and $\bar{k}_p$, $\bar{k}_d$, and $\bar{k}_i$ represent the proportional, derivative, and integral gains, respectively. As in [11] and [15], we use mass-normalized parameters and shifted state variables that facilitate later the construction of Lyapunov functions for the stability analysis

$$k_p := \frac{\bar{k}_p}{m}, \ k_d := \frac{\bar{k}_d + \alpha}{m}, \ k_i := \frac{\bar{k}_i}{m}, \ F_s := \frac{\bar{F}_s}{m}, \ f := \frac{\bar{f}}{m}, \quad (4)$$

$$\hat{x} := \begin{bmatrix} \hat{\sigma} \\ \hat{\phi} \\ \hat{v} \end{bmatrix} := \begin{bmatrix} -k_i(z_1 - r) \\ -k_p(z_1 - r) - k_i z_3 \\ z_2 \end{bmatrix}. \quad (5)$$

Using (4) and (5), model (1)–(3) corresponds to

$$
\begin{aligned}
\dot{\hat{x}} &= \begin{bmatrix} \dot{\hat{\sigma}} \\ \dot{\hat{\phi}} \\ \dot{\hat{v}} \end{bmatrix} \in \begin{bmatrix} -k_i \hat{v} \\ \hat{\sigma} - k_p \hat{v} \\ \hat{\phi} - k_d \hat{v} - F_s \operatorname{Sign}(\hat{v}) + f(\hat{v}) \end{bmatrix} \\
&= \begin{bmatrix} 0 & 0 & -k_i \\ 1 & 0 & -k_p \\ 0 & 1 & -k_d \end{bmatrix} \begin{bmatrix} \hat{\sigma} \\ \hat{\phi} \\ \hat{v} \end{bmatrix} - e_3(F_s \operatorname{Sign}(\hat{v}) - f(\hat{v})) \\
&=: A\hat{x} - e_3(F_s \operatorname{Sign}(\hat{v}) - f(\hat{v})) =: \hat{\mathcal{F}}_x(\hat{x}). \quad (6)
\end{aligned}
$$

Note that $\hat{\sigma}$ is a generalized position error, and $\hat{\phi}$ is the controller state encompassing the proportional and integral control actions.

Let us now adopt the following assumptions on the velocity-dependent friction characteristic f and the controller gains.

Assumption 1: Function $f : \mathbb{R} \to \mathbb{R}$ satisfies the following.
1) $|f(\hat{v})| \le F_s$ for all $\hat{v}$.
2) $\hat{v} f(\hat{v}) \ge 0$ for all $\hat{v}$.
3) f is globally Lipschitz with Lipschitz constant $L > 0$.
4) For some $\varepsilon_v > 0$, $f(\hat{v}) = L_2 \hat{v}$ for all $|\hat{v}| \le \varepsilon_v$.

A possible f satisfying Assumption 1 is depicted in Fig. 1. Items 1–3 are clearly not restrictive for typical friction laws. Since ε_v can be selected arbitrarily small, item 4 is hardly restrictive. Finally, note that any continuous function satisfying Assumption 1 can be considered for f, extending beyond classical Stribeck contributions.

In the new coordinates $\hat{x}$, a solution is said to be in a *stick* or *slip* phase when it belongs, respectively, to the sets

$$\mathcal{E}_{\text{stick}} := \left\{ \hat{x} \in \mathbb{R}^3 : \hat{v} = 0, |\hat{\phi}| \le F_s \right\}, \quad \mathcal{E}_{\text{slip}} := \mathbb{R}^3 \setminus \mathcal{E}_{\text{stick}}. \quad (7)$$

TABLE I
INITIAL CONDITIONS CONSIDERED IN LEMMA 1

$(\hat{v}_0 > 0) \vee (\hat{v}_0 = 0 \wedge \hat{\phi}_0 > F_s)$ $\vee (\hat{v}_0 = 0 \wedge \hat{\phi}_0 = F_s \wedge \hat{\sigma}_0 > 0)$	(8)
$(\hat{v}_0 = 0 \wedge \hat{\sigma}_0 > 0 \wedge \hat{\phi}_0 \in [-F_s, F_s))$ $\vee (\hat{v}_0 = 0 \wedge \hat{\sigma}_0 = 0 \wedge \hat{\phi}_0 \in [-F_s, F_s])$ $\vee (\hat{v}_0 = 0 \wedge \hat{\sigma}_0 < 0 \wedge \hat{\phi}_0 \in (-F_s, F_s])$	(9)
$(\hat{v}_0 < 0) \vee (\hat{v}_0 = 0 \wedge \hat{\phi}_0 < -F_s)$ $\vee (\hat{v}_0 = 0 \wedge \hat{\phi}_0 = -F_s \wedge \hat{\sigma}_0 < 0)$	(10)

Indeed, from Assumption 1, when $\hat{v} = 0$, until $|\hat{\phi}| < F_s$, the only possible evolution in (6) is with $\dot{\hat{v}} = 0$ (a stick phase).

Assumption 2: The control gains k_p, k_d, and k_i satisfy $k_p > 0$, $k_i > 0$, and $k_p k_d > k_i$.

Assumption 2 merely requires (by the Routh–Hurwitz criterion) that matrix A is Hurwitz, i.e., it requires asymptotic stability in the frictionless case $F_s = 0$, $f \equiv 0$. Note that if $k_p < 0$, or $k_i < 0$, or $k_p k_d < k_i$, then A has at least one eigenvalue with positive real part, and the closed loop (6) cannot be globally asymptotically stable (GAS) due to the global boundedness of the term multiplying e_3 [43].

The next lemma provides insight in the evolution of solutions to (6) and will be useful in the subsequent derivations.

Lemma 1: Consider model (6) under Assumptions 1 and 2 and the initial conditions in Table I. The following holds.
1) For each initial condition $\hat{x}_0 \in \mathbb{R}^3$, there exists a unique solution $\hat{x}$ to (6) with $\hat{x}(0) = \hat{x}_0$, which is also complete.
2) For each initial condition $\hat{x}_0 = (\hat{\sigma}_0, \hat{\phi}_0, \hat{v}_0)$ satisfying (8), there exists $T > 0$ such that the unique solution $\hat{x}$ to (6) with $\hat{x}(0) = \hat{x}_0$ coincides over $[0, T]$ with the unique solution $\tilde{x}$ to

$$\dot{\tilde{x}} = A\tilde{x} - e_3(F_s - f(\tilde{v})), \quad \tilde{x}(0) = \hat{x}_0, \quad (11)$$

which satisfies $\tilde{v}(t) > 0$ for all $t \in (0, T]$.
3) For each initial condition $\hat{x}_0 = (\hat{\sigma}_0, \hat{\phi}_0, \hat{v}_0)$ satisfying (9), there exists $T > 0$ such that the unique solution $\hat{x}$ to (6) with $\hat{x}(0) = \hat{x}_0$ coincides over $[0, T]$ with the unique solution $\tilde{x}$ to

$$\dot{\tilde{x}} := \begin{bmatrix} \dot{\tilde{\sigma}} \\ \dot{\tilde{\phi}} \\ \dot{\tilde{v}} \end{bmatrix} = \begin{bmatrix} 0 \\ \hat{\sigma} \\ 0 \end{bmatrix}, \quad \tilde{x}(0) = \hat{x}_0, \quad (12)$$

which satisfies $\tilde{v}(t) = 0$ for all $t \in [0, T]$.
4) For each $\hat{x}_0 = (\hat{\sigma}_0, \hat{\phi}_0, \hat{v}_0)$ satisfying (10), there exists $T > 0$ such that the unique solution $\hat{x}$ to (6) with $\hat{x}(0) = \hat{x}_0$ coincides over $[0, T]$ with the unique solution $\tilde{x}$ to

$$\dot{\tilde{x}} = A\tilde{x} - e_3(-F_s - f(\tilde{v})), \quad \tilde{x}(0) = \hat{x}_0, \quad (13)$$

which satisfies $\tilde{v}(t) < 0$ for all $t \in (0, T]$.

The proof of the lemma, which extends [15, Lemma 1 and Claim 1] for a nonzero f, is omitted due to space constraints but can be found in [12]. We emphasize that the lemma can also be proven using the theory of monotone set-valued operators (see the recent extensive survey [17]). As a matter of fact, the closed loop (6) fits exactly within the class of differential inclusions with maximal monotone set-valued nonlinearities.

Indeed, the set-valued part is $e_3 \text{sign}(e_3^\top \hat{x}) = \partial g(\hat{x})$, which is the gradient of a proper, convex and lower semicontinuous function g so that ∂g is a maximal monotone operator. Hence, well-posedness, continuity with respect to initial conditions, existence of periodic solutions, time-discretization, and stability could be addressed using the tools well surveyed in [17]. Alternative possible frameworks are represented by the impulsive differential inclusions in [8]. Despite these possible alternative representations, we adopt here the hybrid systems framework of [25], which provides powerful Lyapunov-based tools to prove our results.

B. Reset Controller Design

In order to solve Problem 1, we replace the integrator in (3) and (6) with a *reset* integrator. The integrator performs two types of resets whose design is best explained in the *original* coordinates z (instead of $\hat{x}$). The key mechanism of these resets is to enforce that the integrator control force (given by $\bar{k}_i z_3$) always points in the direction of the setpoint, namely

$$z_3(z_1 - r) \geq 0, \tag{14}$$

which imposes an initialization constraint on the integrator state z_3 and is then satisfied along all hybrid solutions of the resulting closed loop. Due to the phase lag associated with a *linear* integrator, property (14) cannot be achieved with a classical PID controller [41, Secs. 1.3 and 2.3.2].

To obtain well-defined reset conditions ensuring (14), we augment the PID controller dynamics with an extra Boolean state $\hat{b} \in \{-1, 1\}$, characterizing whether the mass moves *toward* the setpoint ($\hat{b} = 1$) or *away from* the setpoint ($\hat{b} = -1$, typically occurring after an overshoot of the position error). More precisely, $\hat{b}$ always satisfies

$$\hat{b} z_2 (z_1 - r) \leq 0 \tag{15}$$

along the hybrid solutions. To ensure (15) and also (14), our two types of resets are triggered by a zero crossing of each one of the two factors in (15). The first reset is triggered by the zero-crossing of the position error $z_1 - r$ (marking the start of an overshoot of the position error) and is given by

$$(z_1 - r = 0 \wedge \hat{b} = 1) \implies (z_3^+ = -z_3, \ \hat{b}^+ = -\hat{b}). \tag{16a}$$

Besides the fact that the reset in (16a) is required to obtain stability of the setpoint, it also induces significant overshoot reduction, as illustrated in Section II-C.

The second reset yields a change of the integrator state z_3 to zero when the velocity z_2 hits zero after an overshoot, that is,

$$(z_2 = 0 \wedge \hat{b} = -1) \implies (z_3^+ = 0, \ \hat{b}^+ = -\hat{b}). \tag{16b}$$

The reset in (16b) is required to obtain asymptotic stability of the setpoint. Indeed, if it were absent, this would not allow the integrator state z_3 to decrease in absolute value since (14) forces z_3 and $z_1 - r$ in (3) to always have the same sign [and $\dot{z}_3 = z_1 - r$ from (3)]. A (sufficiently) large initial condition for z_3 would then hinder global asymptotic stability of the setpoint. In summary, the resulting closed-loop system with the proposed reset PID controller is given by (1)–(3), with the resetting laws (16).
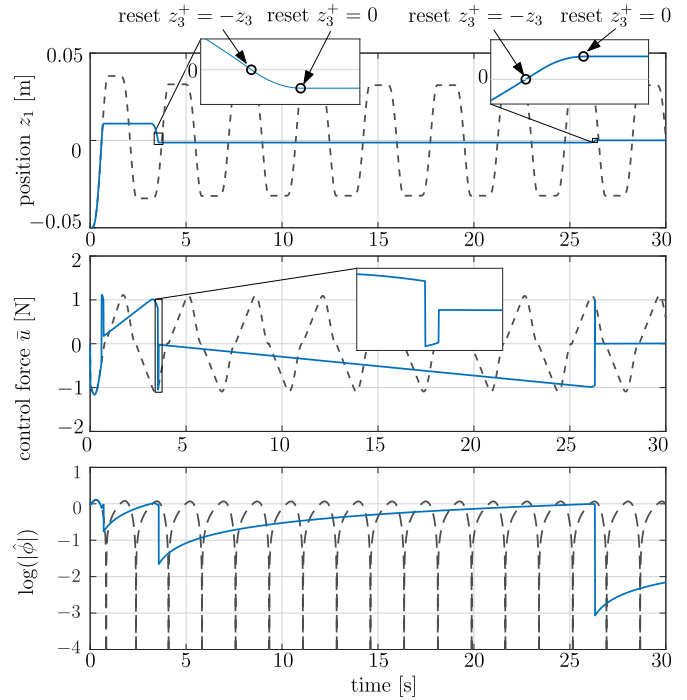

Fig. 2. Simulated response of the position z_1 (top), the control force $\bar{u}$ (middle), and the absolute value of state $\hat{\phi}$ in (5) in the logarithmic scale (bottom) for the classical (− −) and reset (——) PID control schemes.

C. Illustrative Example

We will illustrate the working principle of the proposed reset controller by means of a simulation example, using a numerical time-stepping scheme [2, Ch. 10].

First consider system (1)–(3), where only a *classical* PID controller (3) is employed. The mass m is unitary, the static friction is $\bar{F}_s = 0.981$ N, the viscous friction coefficient α is zero, and the velocity-dependent friction contribution is

$$\bar{f}(z_2) = \begin{cases} L_2 z_2, & |z_2| \leq \varepsilon_v, \\ (\bar{F}_s - \bar{F}_c)\kappa z_2 (1 + \kappa |z_2|)^{-1}, & |z_2| > \varepsilon_v, \end{cases}$$

with $\bar{F}_c = \bar{F}_s/3$ being the Coulomb friction level, $\kappa = 20$ s/m the Stribeck shape parameter, $L_2 = 12.8$ Ns/m, and $\varepsilon_v = 10^{-3}$ m/s, satisfying Assumption 1. We take $\bar{k}_p = 18$ N/m, $\bar{k}_d = 2$ Ns/m, and $\bar{k}_i = 30$ N/(ms), satisfying Assumption 2. The constant setpoint is $r = 0$, and the initial conditions are $z_1(0) = -0.05$ m, $z_2(0) = 0$ m/s, and $z_3(0) = 0$ ms. The position response is presented in the top plot of Fig. 2 (- -), where persistent oscillations (hunting) are evident.

Now, consider the reset closed loop (1)–(3) and (16). The reset controller achieves, first, asymptotic stability of the setpoint $(z_1, z_2) = (r, 0)$ (as proven later) and, second, overshoot reduction compared to the classical PID response [see the top plot of Fig. 2 (− −)]. The insets show the controller resets according to (16a) (i.e., at a zero-crossing of the position error) and according to (16b) (i.e., when the velocity hits zero after the previous reset has occurred). The arising (discontinuous) control force is presented in the middle plot of Fig. 2.

The bottom plot of Fig. 2 is an anticipation for the specific property, established in Section III, that the state $\hat{\phi}$ in (5) never becomes zero when the reset mechanism is active, whereas it

keeps crossing zero for the classical PID (the logarithm of $|\hat{\phi}|$ goes to $-\infty$). Notice that $\hat{\phi}$ is reset according to (16b) at increasingly smaller values ($\hat{\phi}^+ = -k_p(z_1 - r)$) as the state approaches the settling condition $z_1 - r = 0$ and $z_2 = 0$, which is to be expected due to homogeneity of the reset law. Nevertheless, $\hat{\phi}$ never reaches zero (as rigorously established in Proposition 2).

III. MAIN RESULT

A. Hybrid Model Formulation and Stability Theorem

To state our main result, we write the reset closed loop (1)–(3) and (16) using the hybrid formalism of [25]. The resulting hybrid system, denoted by $\hat{\mathcal{H}}$, has an augmented state vector $\hat{\xi}$ ranging in a constrained set comprising a correct initialization of the logic variable $\hat{b}$ and the continuous controller state $\hat{\phi}$

$$\hat{\xi} := (\hat{x}, \hat{b}) := (\hat{\sigma}, \hat{\phi}, \hat{v}, \hat{b}) \in \hat{\Xi}$$

$$\hat{\Xi} := \left\{ (\hat{x}, \hat{b}) \in \mathbb{R}^3 \times \{-1, 1\} : \hat{b}\hat{v}\hat{\sigma} \geq 0, \ \hat{\sigma}\hat{\phi} \geq \frac{k_p}{k_i}\hat{\sigma}^2, \ \hat{b}\hat{v}\hat{\phi} \geq 0 \right\}.$$
(17a)

In $\hat{\Xi}$, the first constraint [inherited from (15)] imposes that $\hat{b}\hat{v}$ and $\hat{\sigma}$ never have opposite signs, while the second constraint [inherited from (14)] imposes that $\hat{\sigma}$ and $\hat{\phi}$ never have opposite signs. With these two constraints in place, one should impose that also $\hat{b}\hat{v}$ and $\hat{\phi}$ never have opposite signs, as ensured by the third constraint characterizing $\hat{\Xi}$.[1]

More specifically, using (4) and (5) to represent (1)–(3), the corresponding closed-loop model (6) augmented with the resets (16) follows the hybrid dynamics:

$$\hat{\mathcal{H}} : \begin{cases} \dot{\hat{\xi}} \in \hat{\mathcal{F}}(\hat{\xi}), & \hat{\xi} \in \hat{\mathcal{C}} := \hat{\Xi} \quad (17b) \\ \hat{\xi}^+ = \begin{cases} \hat{g}_\sigma(\hat{\xi}), & \text{if } \hat{\xi} \in \hat{\mathcal{D}}_\sigma \\ \hat{g}_v(\hat{\xi}), & \text{if } \hat{\xi} \in \hat{\mathcal{D}}_v, \end{cases} & \hat{\xi} \in \hat{\mathcal{D}} := \hat{\mathcal{D}}_\sigma \cup \hat{\mathcal{D}}_v. \quad (17c) \end{cases}$$

Herein, the flow map is given by

$$\hat{\mathcal{F}}(\hat{\xi}) := \begin{bmatrix} -k_i\hat{v} \\ \hat{\sigma} - k_p\hat{v} \\ \hat{\phi} - k_d\hat{v} - F_s\,\mathrm{Sign}(\hat{v}) + f(\hat{v}) \\ 0 \end{bmatrix} = \begin{bmatrix} \hat{\mathcal{F}}_x(\hat{x}) \\ 0 \end{bmatrix} \quad (17d)$$

and the jump maps and jump sets are given by

$$\hat{g}_\sigma(\hat{\xi}) := \begin{bmatrix} \hat{\sigma} \\ -\hat{\phi} \\ \hat{v} \\ -\hat{b} \end{bmatrix}, \quad \hat{g}_v(\hat{\xi}) := \begin{bmatrix} \hat{\sigma} \\ \frac{k_p}{k_i}\hat{\sigma} \\ \hat{v} \\ -\hat{b} \end{bmatrix}, \quad (17e)$$

$$\hat{\mathcal{D}}_\sigma := \left\{ \hat{\xi} \in \hat{\Xi} : \hat{\sigma} = 0, \hat{b} = 1 \right\}, \quad (17f)$$

$$\hat{\mathcal{D}}_v := \left\{ \hat{\xi} \in \hat{\Xi} : \hat{v} = 0, \hat{b} = -1 \right\} \quad (17g)$$

where $\hat{\mathcal{D}}_\sigma$ and $\hat{\mathcal{D}}_v$ are disjoint because they correspond to the two different values of $\hat{b}$. $\hat{g}_\sigma$ and $\hat{\mathcal{D}}_\sigma$ correspond to the resetting mechanism in (16a) and $\hat{g}_v$ and $\hat{\mathcal{D}}_v$ to that in (16b).

Based on formulation (17) of the hybrid closed loop (1)–(3) and (16), we focus for stability of the setpoint on the compact set defined by all possible equilibria of the flow map (17d)

$$\hat{\mathcal{A}} := \left\{ \hat{\xi} \in \hat{\Xi} : \hat{\sigma} = 0, |\hat{\phi}| \leq F_s, \hat{v} = 0 \right\}. \quad (18)$$

[1] Note that the first two constraints in $\hat{\Xi}$ do not imply $\hat{b}\hat{v}\hat{\phi} \geq 0$ because, with $\hat{\sigma} = 0$, the first two constraints are satisfied for any (even opposite and nonzero) selections of $\hat{b}\hat{v}$ and $\hat{\phi}$.

Our main result, stated next, establishes global asymptotic stability of the set of all possible equilibria. This is clearly the smallest possible set that can enjoy global stability properties. The proof of this result is postponed to Sections V and VI to avoid breaking the flow of the exposition.

Theorem 1: Under Assumptions 1 and 2, the set $\hat{\mathcal{A}}$ in (18) is GAS for $\hat{\mathcal{H}}$ in (17).

B. Robustness and Well Posedness Properties

We discuss here robustness properties of the GAS result of Theorem 1. To this end, due to the regularity property established below, the robustness results in [25, Ch. 7] apply, and one can state robust uniform global stability and uniform global attractivity of $\hat{\mathcal{A}}$. Among other things, the semiglobal practical robustness of stability established in [25, Lemma 7.20] reveals that one should expect a graceful performance degradation in the presence of uncertainties, disturbances, and unmodeled phenomena. One nontrivial consequence of robustness is an input-to-state stability result with respect to an input-matched disturbance acting on the dynamics. Proving rigorously this result would go beyond the page limits of this publication but can be done by adapting the local/global bounds constructed in the proof of [15, Proposition 2] and exploiting the uniform boundedness properties established later in Section V. Another important result that we prove below is that the solutions of the closed-loop dynamics (17) are complete (i.e., they evolve forever), namely, they are well behaved.

Proposition 1: The hybrid system (17) satisfies the hybrid basic conditions of [25, Assumption 6.5]. Moreover, under Assumptions 1 and 2, all maximal solutions are complete.

Proof: Verifying the hybrid basic conditions of [25, Assumption 6.5] is straightforward from closedness of sets $\hat{\mathcal{C}}$, $\hat{\mathcal{D}}_\sigma$, and $\hat{\mathcal{D}}_v$ and the regularity properties of $\hat{\mathcal{F}}$, $\hat{g}_\sigma$, and $\hat{g}_v$. To prove completeness of maximal solutions, we apply [25, Proposition 6.10]. To this end, we first prove the existence of nontrivial solutions [25, Definition 2.5] for each $\hat{\xi}_0 = (\hat{\sigma}_0, \hat{\phi}_0, \hat{v}_0, \hat{b}_0) \in \hat{\mathcal{C}} \cup \hat{\mathcal{D}} = \hat{\mathcal{C}} = \hat{\Xi}$. This is straightforward if $\hat{\xi}_0$ is in the interior of $\hat{\mathcal{C}}$. To address the remaining points in $\partial\hat{\mathcal{C}}$ (i.e., the boundary of $\hat{\mathcal{C}}$), we follow a case-by-case proof in the extended version [12]. Here, we provide a shorter proof based on the expression [16, eq. (4.6)] of the tangent cone. Denote the boundaries in $\partial\hat{\mathcal{C}}$ by

$$h_1(\hat{\xi}) := \hat{b}\hat{\sigma}\hat{v} = 0, \quad h_2(\hat{\xi}) := \hat{\sigma}\hat{\phi} - \frac{k_p}{k_i}\hat{\sigma}^2 = 0,$$

$$h_3(\hat{\xi}) := \hat{b}\hat{\phi}\hat{v} = 0,$$

and from [16, eq. (4.6)], we only need to show that for each $i = 1, 2, 3, \hat{\xi} \in \partial\hat{\mathcal{C}} \setminus \hat{\mathcal{D}}$ and $h_i(\hat{\xi}) = 0$ implies $\dot{h}_i(\hat{\xi}) \geq 0$ along one flowing solution. We split the analysis in three cases.

1) *Case 1:* If $h_1(\hat{\xi}) = 0$ (namely, $\hat{\sigma} = 0$ or $\hat{v} = 0$), we obtain along the flow dynamics (17d)

$$\dot{h}_1(\hat{\xi}) = -\hat{b}k_i\hat{v}^2 + \hat{b}\hat{\sigma}\dot{\hat{v}} \in -\hat{b}k_i\hat{v}^2 + \hat{b}\hat{\sigma}(\hat{\phi} + [-F_s, F_s])$$

where the set membership uses $h_1(\hat{\xi}) = 0$. First, consider $\hat{v} = 0$, and notice that $\hat{b} = -1$ implies $\hat{\xi} \in \hat{\mathcal{D}}_v$ (a nontrivial solution jumps). When $\hat{b} = 1$,

then either $\dot{\hat{v}} = 0$ (stick phase), which implies $\dot{h}_1(\hat{\xi}) = 0$, or $\text{sign}(\dot{\hat{v}}) = \text{sign}(\hat{\phi})$ because $\hat{\phi}$ is large enough to overcome the Coulomb friction (slip phase), which implies that $\text{sign}(\dot{h}_1(\hat{\xi})) = \text{sign}(\hat{\sigma}\hat{v}) = \text{sign}(\hat{\sigma}\hat{\phi}) \geq 0$, due to $\hat{\sigma}\hat{\phi} \geq (k_p/k_i)\hat{\sigma}^2$ in (17a). Second, consider $\hat{\sigma} = 0$, and notice that $\hat{b} = 1$ implies $\hat{\xi} \in \hat{\mathcal{D}}_\sigma$ (a nontrivial solution jumps). When $\hat{b} = -1$, then $\dot{h}_1(\hat{\xi}) = k_i\hat{v}^2 \geq 0$.

2) *Case 2:* If $h_2(\hat{\xi}) = 0$ (namely, $\hat{\sigma} = 0$ or $\hat{\phi} = (k_p/k_i)\hat{\sigma}$), we obtain along the flow dynamics (17d)

$$\dot{h}_2(\hat{\xi}) = \hat{\sigma}^2 + k_i\hat{v}\left(\frac{k_p}{k_i}\hat{\sigma} - \hat{\phi}\right).$$

Consider first the case $\hat{\phi} = (k_p/k_i)\hat{\sigma}$, which gives $\dot{h}_2(\hat{\xi}) = \hat{\sigma}^2 \geq 0$. Consider next the case $\hat{\sigma} = 0$ and notice that $\hat{b} = 1$ implies $\hat{\xi} \in \hat{\mathcal{D}}_\sigma$ (a nontrivial solution jumps). When $\hat{b} = -1$, then $\dot{h}_2(\hat{\xi}) = -k_i\hat{v}\hat{\phi} \geq 0$, due to $\hat{b}\hat{v}\hat{\phi} \geq 0$ in (17a).

3) *Case 3:* If $h_3(\hat{\xi}) = 0$ (namely, $\hat{v} = 0$ or $\hat{\phi} = 0$), we obtain along the flow dynamics (17d)

$$\dot{h}_3(\hat{\xi}) = \hat{b}(\hat{\sigma} - k_p\hat{v})\hat{v} + \hat{b}\hat{\phi}\dot{\hat{v}}.$$

The case $\hat{v} = 0$ is dealt with as in Case 1. Next, the case $\hat{\phi} = 0$ implies that $\hat{\sigma} = 0$ due to $\hat{\sigma}\hat{\phi} \geq (k_p/k_i)\hat{\sigma}^2$ in (17a). Since $\hat{\sigma} = 0$, $\hat{b} = 1$ implies that $\hat{\xi} \in \hat{\mathcal{D}}_\sigma$ (a nontrivial solution jumps). When $\hat{b} = -1$, $\dot{h}_3(\hat{\xi}) = k_p\hat{v}^2 \geq 0$.

The proof is completed by noting that case *(b)* of [25, Proposition 6.10] cannot occur because the flow map is a linear system with bounded inputs; hence, flowing solutions are forward complete. Case *(c)* of [25, Proposition 6.10] cannot occur because $\hat{g}_\sigma(\hat{\mathcal{D}}_\sigma) \cup \hat{g}_v(\hat{\mathcal{D}}_v) \subset \hat{\mathcal{C}} \cup \hat{\mathcal{D}}$ as it can be verified through (17e)–(17g). Then, only case *(a)* of [25, Proposition 6.10] remains, i.e., each solution $\hat{\xi}$ is complete. □

C. Experimental Implementation

A relevant property enjoyed by the solutions of (17) is that the transformed controller state $\hat{\phi}$ never reaches zero, unless it is initialized at zero or reaches the attractor $\hat{\mathcal{A}}$ in finite time. This fact, useful in Section IV, was illustrated in Section II-C by the bottom plot of Fig. 2 and is formalized next.

Proposition 2: For $\hat{\mathcal{H}}$ in (17), all solutions $\hat{\xi}$ starting in

$$\hat{\Xi}_0 := \{\hat{\xi} \in \hat{\Xi} : \hat{\phi} \neq 0\} \tag{19}$$

and never reaching $\hat{\mathcal{A}}$ satisfy $\hat{\phi}(t, j) \neq 0 \; \forall \, (t, j) \in \text{dom}\,\hat{\xi}$.

Proof: The proof amounts to showing that no solution evolving in $\hat{\Xi}_0$ can reach a point, where $\hat{\phi} = 0$, after flowing or jumping, unless it reaches $\hat{\mathcal{A}}$.

Consider solutions flowing in $\hat{\mathcal{C}} := \hat{\Xi}$. If a solution reaches $\hat{\phi} = 0$ while flowing in $\hat{\mathcal{C}}$, there necessarily exists a reverse solution starting at $\hat{\xi}_0 = (\hat{\sigma}_0, \hat{\phi}_0, \hat{v}_0, \hat{b}_0) = (0, 0, \hat{v}_0, \hat{b}_0) \in \hat{\Xi}$ (with $\hat{\sigma}_0 = 0$ because of constraint $\hat{\sigma}\hat{\phi} \geq (k_p/k_i)\hat{\sigma}^2$ and $\hat{v}_0 \neq 0$; otherwise, the solution would be in $\hat{\mathcal{A}}$, which is ruled out by assumption) and flowing in backward time according to $-\hat{\mathcal{F}}(\hat{\xi})$ in (17d) while remaining in $\hat{\Xi}$. However, such a reverse solution does not exist as we show next for $\hat{v}_0 > 0$ (the case $\hat{v}_0 < 0$ is analogous). Since $\hat{v}_0 > 0$, $\hat{v}$ remains positive for a small enough backward-time interval, and the backward

dynamics $\dot{\hat{\sigma}} = k_i\hat{v} > 0$ implies that $\hat{\sigma}$ is also positive in that interval. Hence, constraint $\hat{\sigma}\hat{\phi} \geq (k_p/k_i)\hat{\sigma}^2$ in (17a) becomes $h(\hat{\xi}) := \hat{\phi} - (k_p/k_i)\hat{\sigma}$, which is positive for all such sufficiently small times. Let us note that $h(\hat{\xi}_0) = 0$, and in backward time, $\dot{h}(\hat{\xi}) = -\hat{\sigma} + k_p\hat{v} - (k_p/k_i)(k_i\hat{v}) = -\hat{\sigma}$, which is strictly negative for all such sufficiently small *nonzero* times. Then, $h(\hat{\xi})$ would become negative, and the candidate solution would not remain in $\hat{\Xi}$; therefore, its existence is ruled out.

Bearing in mind that solutions cannot reach $\hat{\phi} = 0$ while flowing, unless they reach $\hat{\mathcal{A}}$, we consider then jumps in (17e). No jump from $\hat{\Xi}_0 \cap \hat{\mathcal{D}}_v$ can give $\hat{\phi}^+ = (k_p/k_i)\hat{\sigma} = 0$; otherwise, from the condition $\hat{v} = 0$ in $\hat{\mathcal{D}}_v$, we would obtain $\hat{\xi}^+ \in \hat{\mathcal{A}}$, which is ruled out by assumption. For jumps from $\hat{\Xi}_0 \cap \hat{\mathcal{D}}_\sigma$, the conclusion is obvious since $\hat{\phi}^+ = -\hat{\phi}$. □

Developing further on the result of Proposition 2, we clarify below two possible types of convergence to $\hat{\mathcal{A}}$. These properties will be necessary in the proof of Theorem 1 (which is given in Sections V and VI).

Proposition 3: Each solution $\hat{\xi}$ to (17) is such that the following holds.

1) If it reaches $\hat{\mathcal{A}}$ in finite time, then it remains in $\hat{\mathcal{A}}$ forever (namely, $\hat{\mathcal{A}}$ is strongly forward invariant [25, Definition 6.25]).
2) If it never reaches $\hat{\mathcal{A}}$ (namely, $\hat{\xi}(t, j) \notin \hat{\mathcal{A}}$ for all $(t, j) \in \text{dom}(\hat{\xi})$), then it evolves forever in the t-direction (namely, $\sup_t \text{dom}\,\hat{\xi} = +\infty$).

Proof: Item 1) follows[2] by inspecting all possible solutions starting in $\hat{\mathcal{A}}$, which may flow in $\hat{\mathcal{C}}$ or jump from $\hat{\mathcal{D}}_\sigma$ or $\hat{\mathcal{D}}_v$. When flowing in $\hat{\mathcal{C}} \cap \hat{\mathcal{A}}$, Lemma 1(3) guarantees that $\hat{\sigma}$, $\hat{\phi}$, and $\hat{v}$ stay constant. Across jumps, we have $\hat{g}_\sigma(\hat{\mathcal{A}}) \subset \hat{\mathcal{A}}$; $\hat{g}_v(\hat{\mathcal{A}}) \subset \hat{\mathcal{A}}$, which proves item 1). Proving item 2) requires nontrivial derivations and is done at the end of Section V-B. □

The established desirable properties of the state $\hat{\phi}$ and the convergence to $\hat{\mathcal{A}}$ can be combined with the robustness results discussed in Section III-B to propose an effective experimental implementation of the proposed reset PID laws, as clarified in the next two remarks.

Remark 1: An important consequence of Proposition 3(2) is that no Zeno solutions emerge from model (17) as long as solutions are not in $\hat{\mathcal{A}}$. Ruling out Zeno solutions is key to well representing the core continuous-time behavior of the plant. However, Zeno solutions emerge inside $\hat{\mathcal{A}}$, where frequent and ineffective controller resets may occur in practical implementation (due to measurement noise) *when* the closed-loop evolution gets close to $\hat{\mathcal{A}}$. To avoid ineffective resets, it is then reasonable and advisable to disable the controller resets whenever the velocity $\hat{v}$ and position error $\hat{\sigma}$ are small enough. In particular, resets should be disabled after resetting from $\hat{\mathcal{D}}_v$ because map $\hat{g}_v$ in (17e) ensures that $\hat{\phi}$ is reset to a small value too whenever $\hat{\sigma}$ is small. A small value of $\hat{\phi}$ yields a small value of the control force, compared to the friction force, which generates robustness against other force disturbances.

---

[2]Note that item 1) of Proposition 3 is also implied by the stability of $\hat{\mathcal{A}}$ established in Theorem 1, but, since this item is instrumental to proving Theorem 1 in Section VI-C, we pursue a different proof to avoid circularity.

Remark 2: Due to the regularity properties of the hybrid model, we expect solutions to remain close to nominal ones in the presence of perturbations (as in noisy environments). The presence of measurements noise may hinder the detection of the zero crossings of $\hat{\sigma}$ (for jumping from $\hat{\mathcal{D}}_\sigma$) or the zero crossing of $\hat{v}$ (for jumping from $\hat{\mathcal{D}}_v$). An elegant and effective solution for the robust detection of zero crossing stems from Proposition 2 combined with the observations in Remark 1, ensuring that the resetting mechanism is only active outside $\hat{\mathcal{A}}$. In particular, Proposition 2 ensures that as long as we pick initial conditions in $\hat{\Xi}_0$ (that is, from (19), we do not initialize $\hat{\phi} = -k_p(z_1 - r) - k_i z_3$ at zero[3]), $\hat{\phi}$ never reaches zero. Then, exploiting the inequalities characterizing $\hat{\Xi}$ in (17a), we have that solutions starting in $\hat{\Xi}_0$ remain unchanged if the zero-measure sets $\hat{\mathcal{D}}_\sigma$ and $\hat{\mathcal{D}}_v$ are exchanged for the sets

$$\bar{\mathcal{D}}_\sigma := \{\hat{\xi} : \hat{\sigma}\hat{\phi} \leq 0, \hat{b} = 1\} \tag{20}$$

$$\bar{\mathcal{D}}_v := \{\hat{\xi} : \hat{v}\hat{\phi} \geq 0, \hat{b} = -1\}, \tag{21}$$

which satisfy $\bar{\mathcal{D}}_\sigma \cap \hat{\Xi}_0 = \hat{\mathcal{D}}_\sigma \cap \hat{\Xi}_0$ and $\bar{\mathcal{D}}_v \cap \hat{\Xi}_0 = \hat{\mathcal{D}}_v \cap \hat{\Xi}_0$. Since $\hat{\phi}$ is never zero during the transient from Proposition 2, conditions (20) and (21) are effective at robustly detecting the zero crossings of $\hat{\sigma}$ and $\hat{v}$, respectively. In fact, a reset condition similar to (21) has already been successfully used in [11] to robustly detect a zero crossing of the velocity.

IV. INDUSTRIAL SYSTEM VALIDATION

A. Experimental Setup

We demonstrate the proposed reset controller on an industrial high-precision motion platform consisting of a sample manipulation stage of an electron microscope [45], as shown in Fig. 3. This same setup has been used in [11, Sec. 5] in a lubricant-free configuration. The absence of lubricant generates dominantly Coulomb and viscous friction, thereby not causing instability of the setpoint (which is asymptotically stable, as proven in [15]). However, in standard machine operating conditions, the lubricant must be used to prevent wear and induces a significant Stribeck effect. The corresponding reset-free responses, as shown in Fig. 4, indicate a severe hunting phenomenon (instability), in contrast to the lubricant-free measurements reported in [11, top of Fig. 4] (where the Stribeck effect is hardly present). In these operating conditions, the platform is an ideal testbed for our reset control solution.

The setup consists of a Maxon RE25 dc servo motor ① connected to a spindle ② via a coupling ③ that is stiff in the rotational direction while being flexible in the translational direction. The spindle drives a nut ④, transforming the rotary motion of the spindle to a translational motion of the attached carriage ⑤, with a ratio of $7.96 \cdot 10^{-5}$ m/rad. The position of the carriage is measured by a linear Renishaw encoder ⑥ with a resolution of 1 nm (and a peak noise level of 4 nm). The carriage is connected to the fixed world with a leaf

[3]When starting the controller with a nonzero position error $z_1 - r \neq 0$ (which is typically the case), the requirement $\hat{\phi} \neq 0$ is easily ensured by initializing the integrator state z_3 at zero.
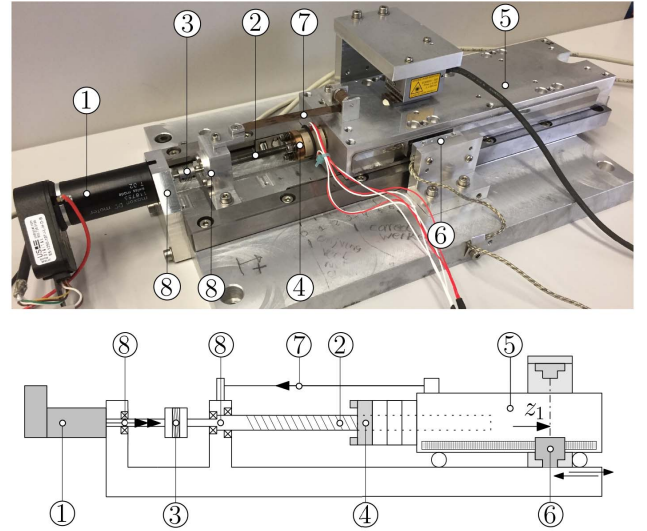

Fig. 3. Experimental setup of a (nanometer) sample manipulation motion stage in an electron microscope [45].

Fig. 4. Responses of position (top), control force (middle), and logarithm of $|\hat{\phi}|$ (bottom) for three experiments with a classical PID controller. The three different colors correspond to three different experiments. The desired accuracy band [(– –) in the top plot] is clearly not achieved with the classical PID controller. The bottom plot shows that $\hat{\phi}$ keeps crossing zero.

spring ⑦, eliminating backlash in the spindle-nut connection. The position accuracy requested by the manufacturer is 10 nm.

For frequencies up to 200 Hz, the dynamics can be well described by (1), for which Theorem 1 applies when using our reset PID controller. In this case, z_1 represents the position of the carriage. The mass $m = 172.6$ kg represents the transformed inertia of motor and spindle (with an *equivalent* mass of 171 kg), plus the mass of the carriage (1.6 kg). Friction is mainly induced by the bearings supporting the motor axis and the spindle (see ⑧ in Fig. 3), by the contact

between the spindle and the nut and, to a lesser extent, by the contact between the carriage and the guidance. The contact between the spindle and the nut is lubricated, which induces the Stribeck effect. Since the system is rigid and behaves like a single mass for frequencies up to 200 Hz, these forces can be summed up to provide the net friction characteristic Ψ in (1).

B. Experiments With Classical PID and Reset PID

Experiments with the classical PID controller (3) have been performed, with gains $\bar{k}_p = 10^7$ N/m, $\bar{k}_d = 2 \cdot 10^3$ Ns/m, and $\bar{k}_i = 10^8$ N/(ms). These satisfy Assumption 2 because from (4), it is enough to check $\bar{k}_p > 0$, $\bar{k}_i > 0$, and $(\bar{k}_p(\bar{k}_d + \alpha))/m > \bar{k}_i$, which hold because $\alpha > 0$ and the gains above satisfy $\bar{k}_p\bar{k}_d/m > \bar{k}_i$. The position response and the corresponding control force are visualized in the top and middle plots of Fig. 4 for three different experiments. Persistent oscillations, and thus the lack of stability of the setpoint, are clearly visible and confirm the presence of a significant Stribeck effect. The bottom plot of Fig. 4 shows that the controller state $\hat{\phi}$ keeps crossing zero (its logarithm becomes negatively unbounded); see also the dashed curve of the lower plot of Fig. 2.

We now employ the proposed reset controller, with the same controller gains as for the classical PID case. We use the reset conditions in (20) and (21) to robustly detect zero crossings of the position error and the velocity, which are equivalent to the next conditions in the physical coordinates z

$$\bar{\mathcal{D}}_\sigma = \left\{(z, \hat{b}) : \bar{k}_i(z_1 - r)\big(\bar{k}_p(z_1 - r) + \bar{k}_i z_3\big) \leq 0, \ \hat{b} = 1\right\}$$
(22a)

$$\bar{\mathcal{D}}_v = \left\{(z, \hat{b}) : z_2\big(\bar{k}_p(z_1 - r) + \bar{k}_i z_3\big) \leq 0, \hat{b} = -1\right\}.$$
(22b)

These sets are independent of the mass m, thereby resulting in a simplified implementation. To avoid ineffective resets triggered by measurement noise according to Remark 1, a stopping criterion is used, which disables resets when the evolution is close to the setpoint. Specifically, resets are disabled whenever the position error is within the desired accuracy band of 10 nm (i.e., $|z_1 - r| \leq 10$ nm) *after a reset from $\bar{\mathcal{D}}_v$* because having a low integral control force compared to the static friction yields robustness to other force disturbances.

Consider Fig. 5, reporting in the top and middle plots the position error and control force for three experiments with the proposed reset controller. For comparison purposes, we enable the controller resets when the PI control force $\hat{\phi}$ and the position error $\hat{\sigma}$ have the same sign, see (17a), after the first zero crossings of the position error. The activation times are indicated by the vertical dashed lines, and before the activation, a classical PID controller with the same tuning is active. The top plot shows that, using the reset enhancements, the system settles within the desired accuracy band of 10 nm after only two resets: the first one from $\bar{\mathcal{D}}_\sigma$ and the second one from $\bar{\mathcal{D}}_v$. The corresponding control force, displayed in the middle subplot, is discontinuous due to the controller resets, as highlighted in the inset. Instead, the classical PID controller does not result in the desired accuracy (see Fig. 4). Also, note that the controller resets from $\bar{\mathcal{D}}_\sigma$ suppress overshoot.
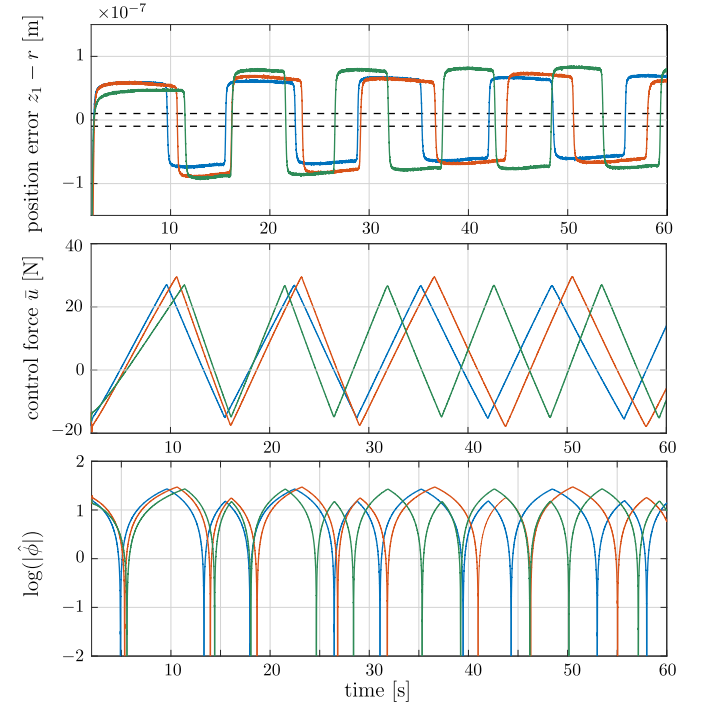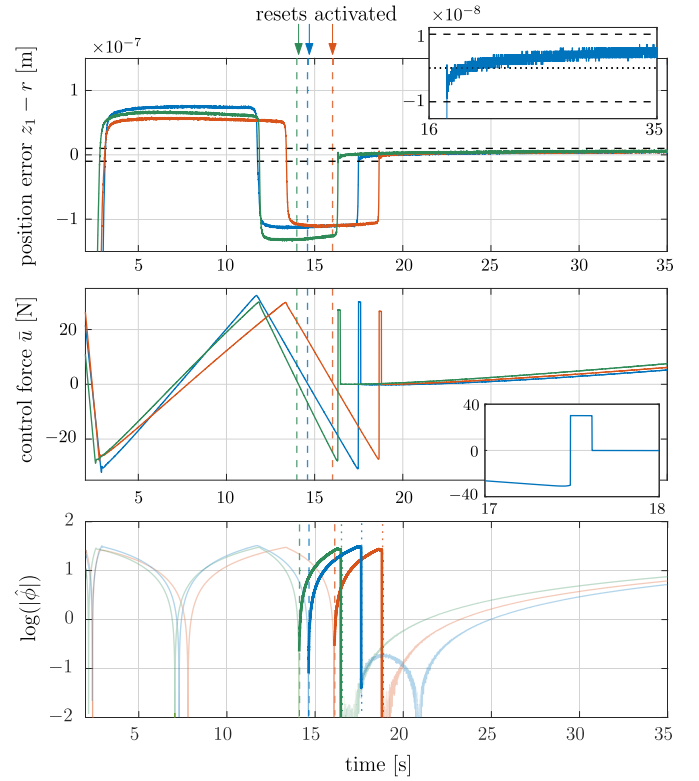

Fig. 5. Responses of position (top), control force (middle), and logarithm of $|\hat{\phi}|$ (bottom) for three experiments with the *reset* PID controller. The three different colors correspond to three different experiments. The bottom plot shows that $\hat{\phi}$ never becomes zero when using resets.

For all three experiments, the desired accuracy is achieved after the first reset from $\bar{\mathcal{D}}_v$. According to Remark 1, the resets are then deactivated (see the vertical dotted lines in the bottom plot). Then, the reset PID is active in the time intervals between the dashed and dotted vertical lines reported in the bottom plot, and those intervals correspond to the darker strokes in that same plot. We note, as indicated in Remark 2, that the reset conditions in the jump sets $\bar{\mathcal{D}}_\sigma$ and $\bar{\mathcal{D}}_v$ correctly trigger the controller reset despite the presence of measurement noise. Indeed, as established in Proposition 2, $\hat{\phi}$ never becomes zero, while the resets are active (see the simulation results in the bottom plot of Fig. 2). Additional insight can be obtained from Fig. 6, where the phase plot without and with resets well illustrates the oscillating response never reaching $\hat{\mathcal{A}}$ (left) and the reset-stabilized response converging to $\hat{\mathcal{A}}$ (right).

Let us now analyze the response at the nanometer scale. Consider the position error response as a result of the controller resets in more detail, using Fig. 7. In this figure, a time interval where $\hat{b} = -1$ is indicated in gray; its boundaries then indicate two reset instants. Conversely, the white areas correspond to intervals where $\hat{b} = 1$. First, consider the top left subplot, which shows a zoomed-in view of the position error of the blue response of Fig. 5. As soon as the error crosses zero at about 17.5 s, a controller reset from $\bar{\mathcal{D}}_\sigma$ is triggered, which toggles the sign of z_3. As a result of stiffness-like effects in the friction characteristic (see [7, Sec. 2.1], [11, Sec. 5]) combined with the sudden (large) change of the control force, a "jump" of the position error is observed, which prevents the
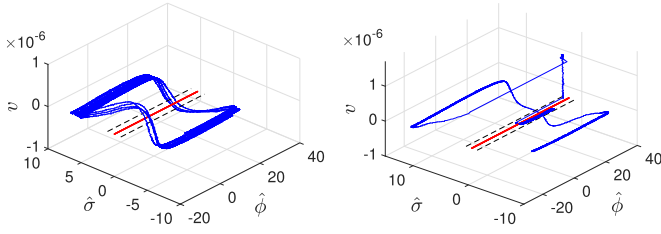
Fig. 6. Phase plot (blue) of the hunting oscillations of Fig. 4 (left) and the reset PID stabilization of Fig. 5 (right). The red segment is an *estimate* of the (unknown) experimental attractor $\hat{\mathcal{A}}$, based on an estimate for the static friction level. The dashed line indicates the desired 10-nm accuracy band.
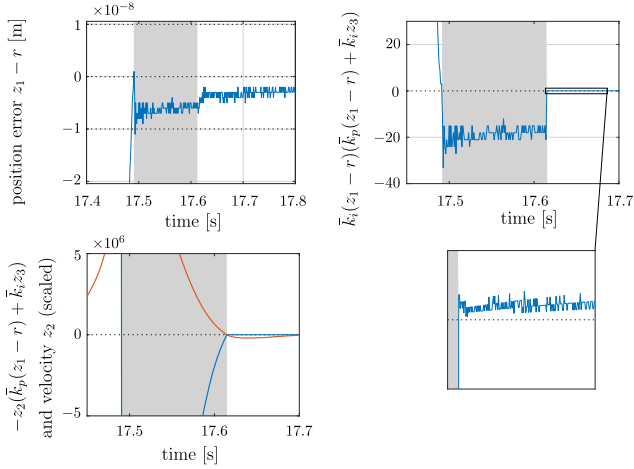

Fig. 7. Zoomed-in view of a position response (top left) and controller reset conditions [top right and bottom left, (——)]. Velocity signal (——).

system from actually overshooting the setpoint. Despite this unmodeled effect, the hysteresis mechanism embedded in $\hat{b}$ prevents an immediate reset from happening again, thus illustrating the robustness properties discussed in Section III-C. Later, at about 17.6 s, a reset from $\bar{\mathcal{D}}_v$ occurs, which resets z_3 to zero. Once again, due to the stiffness effects, a "jump" of the position error occurs (but lower in magnitude, due to the smaller discontinuity in the control force compared to the previous reset from $\bar{\mathcal{D}}_\sigma$). We then observe that the position error crosses zero slowly as a result of frictional creep effects (see [11, Sec. 5.4] and [39]; see [40] for a controller that explicitly deals with such effects); see the inset in the top subplot of Fig. 5. However, the position error remains well within the desired accuracy band of 10 nm, so further resets are disabled according to our stopping criterion.

Next, we analyze the reset conditions in (22a) and (22b) depicted in the top right and bottom left plots of Fig. 7 as a function of time for the blue response in Fig. 5. From the top right plot, it is evident that, indeed, a reset from $\bar{\mathcal{D}}_\sigma$ in (22a) occurs at about 17.5 s when $\hat{b} = 1$ and $\bar{k}_i(z_1 - r)(\bar{k}_p(z_1 - r) + \bar{k}_i z_3) \leq 0$, which is satisfied as soon as the position error crosses zero (see also Fig. 5). Because overshoot is prevented due to the frictional stiffness effects, the reset condition $\bar{k}_i(z_1 - r)(\bar{k}_p(z_1 - r) + \bar{k}_i z_3) \leq 0$ remains true after the reset. However, $\hat{b} = -1$ prevents further resets, which shows that the proposed reset controller exhibits further robustness characteristics with respect to such small-scale

frictional effects. Consider, then, the bottom left plot, and recall that a reset from $\bar{\mathcal{D}}_v$ in (22b) should occur whenever $\hat{b} = -1$ (satisfied because of the occurrence of the previous reset from $\bar{\mathcal{D}}_\sigma$) and when the velocity hits zero. Detecting the latter is successfully done by evaluating the inequality $-z_2(\bar{k}_p(z_1 - r) + \bar{k}_i z_3) \geq 0$ (see also (21) and Remark 2) even though the velocity signal experiences some lag due to the online, noise-reducing low-pass filtering. Since the error $z_1 - r$ is now within the desired accuracy band, the stopping criterion prevents further resets.

V. SEMIGLOBAL PROPERTIES AND SIMULATION MODEL

In this section, we establish a few important stepping stones toward proving Theorem 1. We first show in Section V-A that solutions to (17) are uniformly globally bounded, which enables proving a semiglobal dwell-time property of solutions in Section V-B. Finally, in Section V-C, we define a semiglobal simulation hybrid automaton model in the (bi)simulation sense developed in the computer science context and recently becoming popular in the control community [26]. This model allows proving Theorem 1 in Section VI.

A. Uniform Global Boundedness

Consider the discontinuous Lyapunov-like function

$$W(\hat{\xi}) = \begin{bmatrix} \hat{\sigma} \\ \hat{v} \end{bmatrix}^\top \begin{bmatrix} \frac{k_d}{k_i} & -1 \\ -1 & k_p \end{bmatrix} \begin{bmatrix} \hat{\sigma} \\ \hat{v} \end{bmatrix} + \min_{F \in F_s \, \mathrm{Sign}(\hat{v})} (\hat{b}\hat{\phi} - F)^2 \quad (23)$$

which was used (with $\hat{b} = 1$) in [11, eq. (14)] and [15, eq. (13)] to prove global attractivity with Coulomb friction only. With $\hat{b} = 1$, W can be written and interpreted as a quadratic form in $(\hat{\sigma}, \hat{\phi} - F, \hat{v})$ (with a positive definite matrix by Assumption 2), minimized over all possible values allowed by the set-valued static friction (see [15, p. 2856]).

Due to its discontinuity at points in $\hat{\mathcal{A}}$, the typical (quadratic) upper and lower bounds on W do not hold (in particular, the upper bound does not hold). Therefore, W cannot be used to establish stability but can still be used to prove boundedness of solutions to (17). In particular, for W in (23), it holds that the matrix $\begin{bmatrix} (k_d/k_i) & -1 \\ -1 & k_p \end{bmatrix}$ is positive definite by Assumption 2, and[4] for $\hat{b} \in \{-1, 1\}$, $(\hat{\phi}^2/2) - F_s^2 \leq \min_{F \in F_s \, \mathrm{Sign}(\hat{v})} (\hat{b}\hat{\phi} - F)^2 \leq 2\hat{\phi}^2 + 2F_s^2$. By these inequalities, we construct the bounds

$$W(\hat{\xi}) \leq \bar{c}_W |\hat{x}|^2 + 2F_s^2, \quad |\hat{x}|^2 \leq \underline{c}_W W(\hat{\xi}) + \underline{c}_W F_s^2 \quad (24)$$

for some scalars $\bar{c}_W \geq 1$ and $\underline{c}_W \geq 1$. Bounds (24) show that boundedness of $W(\hat{\xi})$ is equivalent to boundedness of $|\hat{x}|$.

In the presence of Coulomb friction, function W was shown to enjoy useful nonincrease properties in [11] and [15]. These properties were key to proving global attractivity. However, these nonincrease properties are destroyed here due to the velocity-weakening (Stribeck) contribution f in (17d), which was not considered in [11] and [15]. In particular, by defining

$$c_3 := 2(k_p k_d - k_i) > 0 \quad (25)$$

---

[4]The derivation of the next inequalities can be found in [12].

($c_3 > 0$ by Assumption 2), the next lemma provides some useful characterization of the increase/decrease properties of W. Its proof is mostly based on manipulations of the dynamics in the specific sets under consideration and is omitted due to space constraints but can be found in [12].

Lemma 2: Under Assumptions 1 and 2, W in (23) with c_3 in (25) enjoys the following properties along dynamics (17).

1) For each $p \in \{\sigma, \upsilon\}$, we have

$$W\big(g_p(\hat{\tilde{\xi}})\big) - W\big(\hat{\tilde{\xi}}\big) \leq 0 \quad \forall \hat{\tilde{\xi}} \in \mathcal{D}_p. \qquad (26)$$

2) For all $\hat{\tilde{\xi}} = (\hat{\sigma}, \hat{\phi}, \hat{\upsilon}, \hat{b}) \in \mathcal{S}_{\mathcal{H}}$ and each flowing interval $I^j := \{t : (t, j) \in \mathrm{dom}\, \hat{\tilde{\xi}}\}$ with $\hat{b}(t_j, j) = -1$

$$W\big(\hat{\tilde{\xi}}(t_2, j)\big) - W\big(\hat{\tilde{\xi}}(t_1, j)\big) \leq \int_{t_1}^{t_2} -c_3 \hat{\upsilon}(t, j)^2 dt \quad (27)$$

for all $t_1, t_2 \in I^j$ with $t_1 \leq t_2$.

3) There exists a scalar $\bar{W} > 0$ such that each solution $\hat{\tilde{\xi}} = (\hat{\sigma}, \hat{\phi}, \hat{\upsilon}, \hat{b}) \in \mathcal{S}_{\mathcal{H}}$ satisfying $\hat{\tilde{\xi}}(t_j, j-1) \in \mathcal{D}_\upsilon$, jumping to $\hat{\tilde{\xi}}(t_j, j) = \hat{g}_\upsilon(\hat{\tilde{\xi}}(t_j, j-1))$, and then flowing up to $\hat{\tilde{\xi}}(t_{j+1}, j) \in \mathcal{D}_\sigma$ satisfies

$$W\big(\hat{\tilde{\xi}}(t_j, j)\big) \geq \bar{W} \implies W\big(\hat{\tilde{\xi}}(t_{j+1}, j)\big) \leq W\big(\hat{\tilde{\xi}}(t_j, j)\big). \qquad (28)$$

While not being suitable for proving attractivity, function W in (23) and Lemma 2 are useful to prove in the next proposition that solutions to (17) are bounded.

Proposition 4: Under Assumptions 1 and 2, for each compact set $\mathcal{K}$, there exists $M > 0$ such that each solution $\hat{\tilde{\xi}} \in \mathcal{S}_{\mathcal{H}}(\mathcal{K})$ satisfies $\hat{\tilde{\xi}}(t, j) \in M\mathbb{B}$ for all $(t, j) \in \mathrm{dom}\, \hat{\tilde{\xi}}$.

Proof: Consider dynamics (17), and notice that the state $\hat{b}$ is bounded because it evolves in a bounded set. Focusing the attention on the remaining states $\hat{x} = (\hat{\sigma}, \hat{\phi}, \hat{\upsilon})$, their flow obeys the (flow) dynamics in (6), where A is Hurwitz due to Assumption 2, and the term multiplying e_3 is bounded by F_s due to Assumption 1. In particular, from standard bounded-input bounded-output (BIBO) results for linear systems, there exist scalars $k_A \geq 1$ and $h_A > 0$ such that any solution $\hat{\tilde{\xi}} = (\hat{x}, \hat{b})$ satisfies[5]

$$|\hat{x}(t, j)|^2 \leq k_A |\hat{x}(t_j, j)|^2 + h_A \quad \forall t \in [t_j, t_{j+1}] \qquad (29)$$

where $t_0 = 0$, t_j (with $j \geq 1$) denotes a jump time, and possibly $t_{j+1} = +\infty$ with the last flowing interval being open and unbounded. Consider, now, a solution to (17), which may: 1) flow forever (i.e., experiences no jumps); in that case, bound (29) with $j = 0$ provides the desired global bound; 2) exhibit one jump only; in that case, the desired global bound is obtained by concatenating twice bound (29); or 3) flow and/or jump multiple times; in that case, the solution alternately jumps from $\hat{\mathcal{D}}_\sigma$ and $\hat{\mathcal{D}}_\upsilon$ (due to the toggling nature of $\hat{b}$). Hence, the solution jumps from $\hat{\mathcal{D}}_\upsilon$ at either t_1 or (at most) at t_2. Consider the scenario of a first jump happening from $\hat{\mathcal{D}}_\sigma$ at time $(t_1, 0)$, which leads to $|\hat{x}(t_1, 1)|^2 = |\hat{x}(t_1, 0)|^2$ due to $\hat{g}_\sigma$ in (17e), and then a second jump from $\hat{\mathcal{D}}_\upsilon$ at time $(t_2, 1)$, which leads to $|\hat{x}(t_2, 2)|^2 \leq |\hat{x}(t_2, 1)|^2$ due to $\hat{g}_\upsilon$ in

[5]Note that classical BIBO bounds involve the norm not squared, but those are easily extended to (29) by using $(k|x_0| + h)^2 \leq 2k^2|x_0|^2 + 2h^2$.

(17e) and $\hat{\mathcal{D}}_\upsilon$ in (17g) (indeed, $|\hat{\phi}(t_2, 2)| = (k_p/k_i)|\hat{\sigma}(t_2, 1)| \leq |\hat{\phi}(t_2, 1)|$ from constraint $\hat{\sigma}\hat{\phi} \geq (k_p/k_i)\hat{\sigma}^2 \geq 0$ in $\hat{\mathcal{D}}_\upsilon$, which is equivalent to $|\hat{\sigma}||\hat{\phi}| \geq (k_p/k_i)|\hat{\sigma}|^2$). For this described scenario, concatenating bounds yields

$$\max_{(t,j) \in \mathrm{dom}\, \hat{\tilde{\xi}}, t+j \leq t_2+2} |\hat{x}(t, j)|^2 \leq \bar{k}_A |\hat{x}(0, 0)|^2 + \bar{h}_A \qquad (30)$$

where we used $\bar{k}_A := k_A^2 \geq k_A \geq 1$, $\bar{h}_A := h_A(1 + k_A) \geq h_A$. This described scenario can be viewed as the worst-case scenario because bound (30) also applies to the other scenario where the jump from $\hat{\mathcal{D}}_\sigma$ does not occur and the jump from $\hat{\mathcal{D}}_\upsilon$ occurs at t_1 because $\bar{k}_A \geq k_A$ and $\bar{h}_A \geq h_A$. Then, we can consider only this described worst-case scenario without loss of generality. Inequality (30), hence, establishes a uniform bound for all solutions, until a first jump from $\hat{\mathcal{D}}_\upsilon$.

To complete the proof, we must establish a uniform bound on solutions performing a jump from $\hat{\tilde{\xi}}(t_2, 1) \in \hat{\mathcal{D}}_\upsilon$. To this end, we use bounds (24) with (29) to arrive at

$$W\big(\hat{\tilde{\xi}}(t, j)\big) \leq k_W W\big(\hat{\tilde{\xi}}(t_j, j)\big) + h_W \quad \forall t \in [t_j, t_{j+1}] \quad (31)$$

along any flowing solution, where $k_W := \bar{c}_W \underline{c}_W k_A \geq 1$ (since $\bar{c}_W \geq 1$, $\underline{c}_W \geq 1$, and $k_A \geq 1$) and $h_W := \bar{c}_W(k_A \underline{c}_W F_s^2 + h_A) + 2F_s^2 > 0$.

We are now ready to complete bound (30) beyond hybrid time $(t_2, 2)$. We can focus on solutions exhibiting infinitely many jumps without loss of generality, by noting that the analysis also applies to solutions that eventually stop jumping, because the last bound established below in (34) and (35) will hold on the last (unbounded) flowing interval. Given any such solution $\hat{\tilde{\xi}}$ that keeps exhibiting jumps, denote

$$W_0 := W\big(\hat{\tilde{\xi}}(t_2, 2)\big) \leq \bar{c}_W\Big(\bar{k}_A |\hat{x}(0, 0)|^2 + \bar{h}_A\Big) + 2F_s^2 \quad (32)$$

where we combined (30) and (24). Due to the toggling nature of $\hat{b}$ in dynamics (17), jumps must occur alternatively from $\hat{\mathcal{D}}_\upsilon$ at times $(t_2, 1)$, $(t_4, 3)$, and so on (i.e., at jump times $t_2, t_4, \ldots$ with even indices) and from $\hat{\mathcal{D}}_\sigma$ at jump times with odd indices. We proceed by induction. Assume that, at time $(t_{2i}, 2i)$ (after a jump from $\hat{\mathcal{D}}_\upsilon$), we have

$$W\big(\hat{\tilde{\xi}}(t_{2i}, 2i)\big) \leq \max\{k_W \bar{W} + h_W, W_0\}, \qquad (33)$$

which is true for $i = 1$ (the base case of induction) because of (32). As for the induction step, (31) yields for $j = 2i$

$$W\big(\hat{\tilde{\xi}}(t, 2i)\big) \leq k_W W\big(\hat{\tilde{\xi}}(t_{2i}, 2i)\big) + h_W \quad \forall t \in [t_{2i}, t_{2i+1}]. \quad (34)$$

We obtain that $W(\hat{\tilde{\xi}}(t_{2i+1}, 2i)) \leq \max\{k_W \bar{W} + h_W, W(\hat{\tilde{\xi}}(t_{2i}, 2i))\}$ because, for $W(\hat{\tilde{\xi}}(t_{2i}, 2i)) < \bar{W}$, it holds that $W(\hat{\tilde{\xi}}(t_{2i+1}, 2i)) \leq k_W \bar{W} + h_W$ by (34), and for $W(\hat{\tilde{\xi}}(t_{2i}, 2i)) \geq \bar{W}$, it holds that $W(\hat{\tilde{\xi}}(t_{2i+1}, 2i)) \leq W(\hat{\tilde{\xi}}(t_{2i}, 2i))$ by (28) in Lemma 2. Then, $W(\hat{\tilde{\xi}}(t_{2i+1}, 2i)) \leq \max\{k_W \bar{W} + h_W, W(\hat{\tilde{\xi}}(t_{2i}, 2i))\}$ can be propagated to the subsequent time interval using the nonincrease properties of W established in (26) and (27) of Lemma 2, as follows:

$$W\big(\hat{\tilde{\xi}}(t, 2i+1)\big) \leq \max\{k_W \bar{W} + h_W, W\big(\hat{\tilde{\xi}}(t_{2i}, 2i)\big)\}$$
$$\forall t \in [t_{2i+1}, t_{2(i+1)}]. \quad (35)$$

Finally, using again the nonincrease property in (26) and bound (33) for $j = 2i$, we obtain

$$W\big(\hat{\bar{\xi}}\big(t_{2(i+1)}, 2(i+1)\big)\big) \leq \max\big\{k_W \bar{W} + h_W, W\big(\hat{\bar{\xi}}(t_{2i}, 2i)\big)\big\}$$
$$\leq \max\big\{k_W \bar{W} + h_W, W_0\big\}.$$

This corresponds to (33), completes the induction proof, and establishes that (33) holds for all $i \geq 1$.

Summarizing, we combine bounds (34) and (35) [and then use $k_W \geq 1$, $h_W > 0$, (33), and, finally, (32)] to obtain for all $(t, j) \in \mathrm{dom}\,\hat{\bar{\xi}}$ with $t + j \geq t_2 + 2$

$$W\big(\hat{\bar{\xi}}(t, j)\big) \leq \max\Big\{k_W\big(k_W \bar{W} + h_W\big) + h_W,$$
$$k_W\Big(\bar{c}_W\Big(\bar{k}_A|\hat{x}(0,0)|^2 + \bar{h}_A\Big) + 2F_s^2\Big) + h_W\Big\}.$$

In other words, W remains uniformly bounded, so does $\hat{x}$ by (24), and $\hat{\bar{\xi}}$ (since $\hat{b}$ evolves in $\{-1, 1\}$), and the proof of uniform boundedness of solutions is completed. $\qquad\square$

B. Semiglobal Dwell Time

Now we establish a second useful property of solutions of $\hat{\mathcal{H}}$, whose stick-to-slip transitions must occur at instants of time separated by a guaranteed dwell time. This particular dwell time is uniform in any compact set of initial conditions; therefore, it is semiglobal.

To formalize our dwell-time result, define the sets

$$\hat{\mathcal{S}}_1 := \big\{\hat{\bar{\xi}} \in \hat{\Xi} : \hat{\phi} \geq F_s, \hat{v} = 0, \hat{b} = 1\big\}$$
$$\hat{\mathcal{S}}_{-1} := \big\{\hat{\bar{\xi}} \in \hat{\Xi} : \hat{\phi} \leq -F_s, \hat{v} = 0, \hat{b} = 1\big\}$$
$$\hat{\mathcal{S}}_0 := \Big\{\hat{\bar{\xi}} \in \hat{\Xi} : \hat{\phi} = \frac{k_p}{k_i}\hat{\sigma}, |\hat{\phi}| < F_s, \hat{v} = 0, \hat{b} = 1\Big\}. \quad (36)$$

The first two are intuitively associated with stick-to-slip transitions [see (7)], and the third one completes the image of $\hat{\mathcal{D}}_v$ through $\hat{g}_v$. We show in the next proposition that any solution visiting these sets enjoys a uniform semiglobal dwell time before its velocity changes sign, unless it reaches the attractor $\hat{\mathcal{A}}$, where it will remain due to Proposition 3(1).

Proposition 5: Let Assumptions 1 and 2 hold. For each compact set $\mathcal{K}$, there exists $\delta(\mathcal{K}) > 0$ such that each solution $\hat{\bar{\xi}} = (\hat{\sigma}, \hat{\phi}, \hat{v}, \hat{b}) \in \mathcal{S}_{\hat{\mathcal{H}}}(\mathcal{K})$ with $\hat{\bar{\xi}}(t, j) \in \hat{\mathcal{S}}_1 \cup \hat{\mathcal{S}}_{-1} \cup \hat{\mathcal{S}}_0$ satisfies either: 1) $\hat{\bar{\xi}}(t', j') \in \hat{\mathcal{A}}$ for some $t' \in [t, t+\delta(\mathcal{K})]$ or 2) if case 1 does not hold, then, for each $\tau \in [t, t+\delta(\mathcal{K})]$, we have $(\tau, j(\tau)) \in \mathrm{dom}\,\hat{\bar{\xi}}$ and

$$\hat{\bar{\xi}}(t, j) \in \hat{\mathcal{S}}_1 \implies \hat{v}(\tau, j(\tau)) \geq 0$$
$$\hat{\bar{\xi}}(t, j) \in \hat{\mathcal{S}}_{-1} \implies \hat{v}(\tau, j(\tau)) \leq 0$$

for all such $\tau \in [t, t+\delta(\mathcal{K})]$.

To the end of proving Proposition 5, we state the next lemma, where L_2 is defined in Assumption 1(4). The straightforward proof of the lemma is based on the regularity of the right-hand side of (11), is omitted due to space constraints but can be found in [12].

Lemma 3: Let Assumptions 1 and 2 hold.

1) For each $M > 0$, there exists $\delta_0(M) > 0$ such that, for each initial condition $\tilde{x}_0 = (\tilde{\sigma}_0, \check{\phi}_0, 0) \in M\mathbb{B}$, the unique solution $\tilde{x}$ (with $\tilde{x}(0) = \tilde{x}_0$) to (11) coincides over

$[0, \delta_0(M)]$ with the unique solution $\check{x}$ (with $\check{x}(0) = \tilde{x}_0$) to

$$\dot{\check{x}} = A\check{x} - e_3(F_s - L_2\check{v}). \quad (37)$$

2) There exists $\delta_1 > 0$ such that, for each initial condition $\check{x}_0 = (\check{\sigma}_0, \check{\phi}_0, 0)$ with

$$\check{\sigma}_0 \geq 0, \check{\phi}_0 \geq F_s, \begin{bmatrix} \check{\sigma}_0 \\ \check{\phi}_0 \end{bmatrix} \neq \begin{bmatrix} 0 \\ F_s \end{bmatrix} \quad (38)$$

$\big(\check{\sigma}_0 \leq 0, \check{\phi}_0 \leq -F_s, \begin{bmatrix} \check{\sigma}_0 \\ \check{\phi}_0 \end{bmatrix} \neq \begin{bmatrix} 0 \\ -F_s \end{bmatrix}$, respectively$\big)$, the unique solution $\check{x}$ (with $\check{x}(0) = \check{x}_0$) to (37) satisfies for all $t \in (0, \delta_1]$, $\check{v}(t) > 0$, and $\check{\phi}(t) > F_s$ ($\check{v}(t) < 0$ and $\check{\phi}(t) < -F_s$, respectively).

Proof of Proposition 5: Consider first the case $\hat{\bar{\xi}}(t, j) \in \hat{\mathcal{S}}_1$. If $\hat{\bar{\xi}}(t, j) = (0, F_s, 0, 1) \in \hat{\mathcal{S}}_1$, $\hat{\bar{\xi}}(t, j) = (0, F_s, 0, 1) \in \hat{\mathcal{A}}$, and the solution satisfies case 1 of the proposition. We consider then $\hat{\bar{\xi}}(t, j) \neq (0, F_s, 0, 1)$ in the rest of the proof.

By Proposition 4, for each compact set $\mathcal{K}$, there exists $M > 0$ such that, for all $(t, j) \in \mathrm{dom}\,\hat{\bar{\xi}}$ when $\hat{\bar{\xi}}(t, j) \in \hat{\mathcal{S}}_1$, $\hat{\bar{\xi}}(t, j) \in \hat{\mathcal{S}}_1 \cap M\mathbb{B}$. Define $\delta'(\mathcal{K}) := \min\{\delta_0(M), \delta_1\} > 0$, with $\delta_0(M)$ and δ_1 as in Lemma 3.

Evolution With Only Flow: Suppose that $\hat{\bar{\xi}} = (\hat{x}, \hat{b})$ with $\hat{\bar{\xi}}(t, j) \in \hat{\mathcal{S}}_1 \setminus \{(0, F_s, 0, 1)\} \cap M\mathbb{B}$ flows on $[t, t+\delta'(\mathcal{K})]$.

Since $\hat{\bar{\xi}}(t, j) \in \hat{\mathcal{S}}_1 \setminus \{(0, F_s, 0, 1)\} \cap M\mathbb{B}$, it holds that $\hat{x}(t, j) = (\hat{\sigma}(t, j), \hat{\phi}(t, j), 0) \in M\mathbb{B}$. Then, Lemma 3(1) ensures that the unique solution $\tilde{x}$ [with $\tilde{x}(t) = \hat{x}(t, j)$] to (11) coincides over the interval $[t, t+\delta'(\mathcal{K})]$ with the unique solution $\check{x}$ [with $\check{x}(t) = \hat{x}(t, j)$] to (37), which is such that $\check{v}(\tau) > 0$ and $\check{\phi}(\tau) > F_s$ for all $\tau \in [t, t+\delta'(\mathcal{K})]$ by Lemma 3(2) because $\check{x}(t) = \hat{x}(t, j)$ satisfies (38) (by combining conditions $\hat{\phi} \geq F_s$ and $\hat{\sigma}\hat{\phi} \geq (k_p/k_i)\hat{\sigma}^2 \geq 0$ in $\hat{\mathcal{S}}_1$).

Since $\hat{\bar{\xi}}$ flows according to (17d), its component $\hat{x}$ satisfies (6). Solutions to (6) are unique by Lemma 1(1). Since $\tilde{x}$ satisfies the conditions in (8) for all $\tau \in [t, t+\delta'(\mathcal{K})]$, the component $\hat{x}$ of $\hat{\bar{\xi}}$ must coincide with $\tilde{x}$ on the interval $[t, t+\delta'(\mathcal{K})]$. Hence, $(\tau, j(\tau)) \in \mathrm{dom}\,\hat{\bar{\xi}}$, $\hat{v}(\tau, j(\tau)) \geq 0$, and $\hat{\phi}(\tau, j(\tau)) \geq F_s$ for all $\tau \in [t, t+\delta'(\mathcal{K})]$, so the solution $\hat{\bar{\xi}}$ satisfies case 2 of the proposition.

Evolution With Flow and Jumps: The only other possible evolution of $\hat{\bar{\xi}}$ entails a jump from $\hat{\mathcal{D}}_\sigma$ for some $\tau_1 \in [t, t+\delta'(\mathcal{K})]$ such that $\hat{\sigma}(\tau_1, j) = 0$ [the solution $\hat{\bar{\xi}}$ cannot jump from $\hat{\mathcal{D}}_v$ due to $\hat{b}(t, j) = 1$ and $\dot{b} = 0$ in (17d)]. Since $[t, \tau_1] \subset [t, t+\delta'(\mathcal{K})]$, we know from "*Evolution with only flow*" above that $\hat{v}(\tau_1, j) \geq 0$ and $\hat{\phi}(\tau_1, j) \geq F_s$ if $\hat{\bar{\xi}}$ flows in $\hat{\mathcal{C}}$ before jumping from $\hat{\mathcal{D}}_\sigma$. Then, by $\hat{g}_\sigma$ in (17e), $\hat{\sigma}(\tau_1, j+1) = \hat{\sigma}(\tau_1, j) = 0$, $\hat{\phi}(\tau_1, j+1) = -\hat{\phi}(\tau_1, j) \leq -F_s$, $\hat{v}(\tau_1, j+1) = \hat{v}(\tau_1, j) \geq 0$, and $\hat{b}(\tau_1, j+1) = -\hat{b}(\tau_1, j) = -1$. Define τ_2 as the time $\tau_2 \geq \tau_1$ such that

$$\hat{v}(\tau, j+1) > 0 \quad \text{for all } \tau \in (\tau_1, \tau_2), \text{ and } \hat{v}(\tau_2, j+1) = 0. \quad (39)$$

Note that $\tau_2 = \tau_1$ is not excluded. The solution $\hat{\bar{\xi}}$ can only flow on (τ_1, τ_2) since, with $\hat{b}(\tau_1, j+1) = -1$, jumps can only occur from $\hat{\mathcal{D}}_v$ where $\hat{v}$ has to be 0. Moreover, from (39), for

all $\tau \in [\tau_1, \tau_2]$

$$\hat{\sigma}(\tau, j+1) = \hat{\sigma}(\tau_1, j+1) + \int_{\tau_1}^{\tau} -k_i \hat{v}(\tilde{\tau}, j+1) d\tilde{\tau} \leq 0$$

$$\hat{\phi}(\tau, j+1) = \hat{\phi}(\tau_1, j+1) + \int_{\tau_1}^{\tau} \left(\hat{\sigma}(\tilde{\tau}, j+1) - k_p \hat{v}(\tilde{\tau}, j+1) \right) d\tilde{\tau}$$

$$\leq \hat{\phi}(\tau_1, j+1) \leq -F_s$$

hence

$$\hat{v}(\tau_2, j+1) = 0, \ \hat{\sigma}(\tau_2, j+1) \leq 0$$
$$\hat{\phi}(\tau_2, j+1) \leq -F_s, \ \begin{bmatrix} \hat{\sigma}(\tau_2, j+1) \\ \hat{\phi}(\tau_2, j+1) \end{bmatrix} \neq \begin{bmatrix} 0 \\ -F_s \end{bmatrix} \quad (40)$$

where the solution satisfies case (1) of the proposition in case $\begin{bmatrix} \hat{\sigma}(\tau_2, j+1) \\ \hat{\phi}(\tau_2, j+1) \end{bmatrix} = \begin{bmatrix} 0 \\ -F_s \end{bmatrix}$.

We rule out the possibility that $\hat{\xi}$ flows from (40) at $(\tau_2, j+1)$. Indeed, if $\hat{\xi}$ flowed, there would exist $T > 0$ by Lemma 1(4) such that the component $\hat{x}$ of $\hat{\xi}$ coincides over $[\tau_2, \tau_2 + T]$ with the unique solution $\tilde{x}$ to (13) with $\tilde{x}(\tau_2) = \hat{x}(\tau_2, j+1)$, which satisfies $\tilde{v}(\tau) < 0$ for all $\tau \in (\tau_2, \tau_2 + T]$. Such a flowing evolution, however, is not possible because the condition $\hat{b}\hat{v}\hat{\phi} \geq 0$ would be violated on $(\tau_2, \tau_2+T]$ (shrink T if needed) since $\hat{b}(\tau_2, j+1) = -1$. Then, completeness of maximal solutions in Proposition 1 concludes that the only possible evolution from (40) at $(\tau_2, j+1)$ is a jump from $\hat{\mathcal{D}}_v$.

Now, consider two cases for $\hat{\sigma}(\tau_2, j+1)$ in (40) by defining

$$\hat{\sigma}_{\text{th}} := \frac{F_s}{2} \frac{k_i}{k_p} > 0 \quad \text{and} \quad \delta'' := \frac{F_s}{2\hat{\sigma}_{\text{th}}} = \frac{k_p}{k_i} > 0 \quad (41)$$

by Assumption 2.

Evolution With Flow and Jumps: $\hat{\sigma}(\tau_2, j+1) \in [-\hat{\sigma}_{\text{th}}, 0]$: By $\hat{g}_v$ in (17e), $\hat{\sigma}(\tau_2, j+2) = \hat{\sigma}(\tau_2, j+1) \in [-\hat{\sigma}_{\text{th}}, 0]$, $\hat{\phi}(\tau_2, j+2) = (k_p/k_i)\hat{\sigma}(\tau_2, j+1) \in [-(F_s/2), 0]$, and $\hat{b}(\tau_2, j+2) = 1$. If $\hat{\sigma}(\tau_2, j+2) = 0$, then the solution satisfies case (1) of the proposition. Otherwise, no jump can occur over $[\tau_2, \tau_2 + \delta'']$ with δ'' in (41), and $\hat{v}(\tau, j+2) = 0$ for all $\tau \in [\tau_2, \tau_2 + \delta'']$ by Lemma 1(3). Then, $(\tau, j(\tau)) \in \text{dom}\,\hat{\xi}$ and $\hat{v}(\tau, j(\tau)) \geq 0$ for all $\tau \in [t, \tau_2 + \delta'']$ (with $\tau_2 \geq t$ from before), so the solution satisfies case (2) of the proposition.

Evolution With Flow and Jumps: $\hat{\sigma}(\tau_2, j+1) \in (-\infty, -\hat{\sigma}_{\text{th}})$: Recall that $\hat{\sigma}(\tau_1, j+1) = 0$, and note that, for all $\tau \in [\tau_1, \tau_2]$

$$|\dot{\hat{\sigma}}(\tau, j+1)| \leq |\dot{\hat{x}}(\tau, j+1)| \leq |A|M + F_s$$

from (17d), Assumption 1, and Proposition 4. Hence, from $\hat{\sigma}(\tau_2, j+1) = \hat{\sigma}(\tau_1, j+1) + \int_{\tau_1}^{\tau_2} \dot{\hat{\sigma}}(\tau, j+1) d\tau = \int_{\tau_1}^{\tau_2} \dot{\hat{\sigma}}(\tau, j+1) d\tau$, we have

$$|\hat{\sigma}(\tau_2, j+1)| \leq (|A|M + F_s)(\tau_2 - \tau_1). \quad (42)$$

Since $|\hat{\sigma}(\tau_2, j+1)| \geq \hat{\sigma}_{\text{th}}$, (42) implies that

$$(|A|M + F_s)(\tau_2 - \tau_1) \geq \hat{\sigma}_{\text{th}}$$

$$\iff \tau_2 - \tau_1 > \frac{\hat{\sigma}_{\text{th}}}{|A|M + F_s} =: \delta'''(\mathcal{K}) > 0.$$

Then, $(\tau, j(\tau)) \in \text{dom}\,\hat{\xi}$ and $\hat{v}(\tau, j(\tau)) \geq 0$ for all $\tau \in [t, \tau_1 + \delta'''(\mathcal{K})]$ (with $\tau_1 \geq t$ from before), so the solution satisfies case (2) of the proposition.

The proof of the case $\hat{\xi}(t, j) \in \hat{\mathcal{S}}_1$ is completed by selecting $\delta(\mathcal{K}) := \min\{\delta'(\mathcal{K}), \delta'', \delta'''(\mathcal{K})\} > 0$. The case $\hat{\xi}(t, j) \in \hat{\mathcal{S}}_{-1}$ follows parallel arguments and is omitted.

Consider, now, the case $\hat{\xi}(t, j) \in \hat{\mathcal{S}}_0$, which is only sketched because the proof is similar in nature to the previous one but simpler. In this case, two things may happen: either $|\hat{\phi}| = (k_p/k_i)|\hat{\sigma}|$ is smaller than $(F_s/2)$ and then the solution must remain in a stick phase from where it cannot jump (because jumps only from $\hat{\mathcal{D}}_\sigma$ are allowed with $\hat{b} = 1$, and these jumps would bring the solution to $\hat{\mathcal{A}}$, verifying directly case 1 of the proposition); or $|\hat{\phi}| = (k_p/k_i)|\hat{\sigma}|$ is not smaller than $(F_s/2)$, which implies that no jump can happen before some uniform amount of time because $|\hat{\sigma}|$ is bounded away from zero, and $\dot{\hat{\sigma}}$ is bounded.

Based on the previous results, we are now ready to complete the missing proof of item (2) of Proposition 3.

Proof of Item (2) of Proposition 3: The proof uses Propositions 1 and 5. In particular, each solution starts in some compact set $\mathcal{K}$, and after any jump from $\hat{\mathcal{D}}_v$, it lands in the set $\hat{\mathcal{S}}_1 \cup \hat{\mathcal{S}}_{-1} \cup \hat{\mathcal{S}}_0$. From this set, Proposition 5 implies that it flows for some uniform time interval $\delta(\mathcal{K})$ (unless it reaches $\hat{\mathcal{A}}$ and nothing needs to be proven). Due to the hysteresis mechanism enforced by the toggling $\hat{b}$, jumps are alternating from $\hat{\mathcal{D}}_v$, and $\hat{\mathcal{D}}_\sigma$ and the guaranteed flow $\delta(\mathcal{K})$ after each jump from $\hat{\mathcal{D}}_v$ implies that these solutions (which are complete due to Proposition 1) flow forever. Similarly, any solution performing a finite number of jumps must flow forever due to Proposition 1.

C. Semiglobal Simulation by Hybrid Automaton

Based on the results of Section V-B and inspired by the proof given in [14] for the case of only Coulomb friction, we now introduce a hybrid model being semiglobally similar to (17) in the sense of [48, Definition 2.5] (see also [36]). This model is the key tool used in Section VI to prove Theorem 1. More specifically, by recalling the (arbitrarily large) compact set $\mathcal{K}$ discussed in Section V-B (see Proposition 5), the simulation model is parametric in $\delta > 0$ capturing the $\delta(\mathcal{K})$ of Section V-B, and from Proposition 5, we can prove that its outputs are semiglobally coincident with the solutions to (17). This similarity property allows proving Theorem 1 because, for each $\delta > 0$, the simulation model admits an intuitive and elegant Lyapunov function certifying asymptotic stability. Inspired by the hybrid automaton model of Coulomb friction presented in [14], we introduce the simulation model $\mathcal{H}_\delta$ parameterized by $\delta > 0$. The overall state of $\mathcal{H}_\delta$ is

$$\xi := (\sigma, \phi, v, b, q, \tau) \in \Xi$$
$$\Xi := \Big\{ \xi \in \mathbb{R}^3 \times \{-1, 1\} \times \{-1, 0, 1\} \times [0, 2\delta] :$$
$$qv \geq 0, bq\sigma \geq 0, \sigma\phi \geq \frac{k_p}{k_i}\sigma^2, bq\phi \geq 0 \Big\}. \quad (43a)$$

With respect to the state $\hat{\xi}$ of $\hat{\mathcal{H}}$ in (17), we add the logical state $q \in \{-1, 0, 1\}$ (whose sign is never opposite to the sign of v due to the constraints in Ξ) and the timer τ, ranging in the compact set $[0, 2\delta]$. The constrained dynamics of $\mathcal{H}_\delta$ are

$$\mathcal{H}_\delta : \begin{cases} \dot{\xi} = \mathcal{F}(\xi), & \xi \in \mathcal{C}_{\text{slip}} \cup \mathcal{C}_{\text{stick}} & (43b) \\ \xi^+ \in \mathcal{G}(\xi), & \xi \in \bigcup_{p \in \{\sigma, v, 0, 1, -1\}} \mathcal{D}_p. & (43c) \end{cases}$$
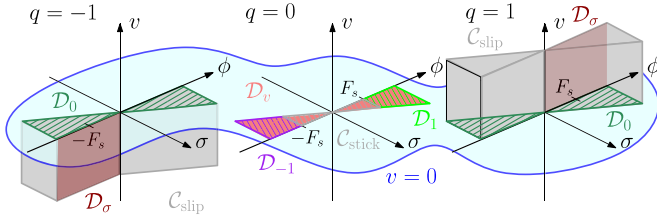
Fig. 8. Projections to the (σ, ϕ, v) space of the flow and jump sets in (43f), indicating the sector condition $\sigma\phi \geq (k_p/k_i)\sigma^2$.
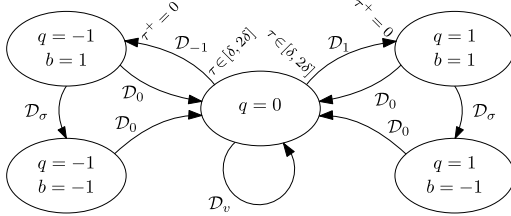

Fig. 9. Hybrid-automaton illustration of (43).

The flow and jump maps $\mathcal{F}$ and $\mathcal{G}$ of $\mathcal{H}_\delta$ are defined as

$$\mathcal{F}(\xi) := \begin{bmatrix} -k_i v \\ \sigma - k_p v \\ -k_d v + |q|\phi - q(F_s - |f(v)|) \\ 0 \\ 0 \\ 1 - \mathrm{dz}_1(\tau/\delta) \end{bmatrix}, \qquad (43\text{d})$$

$$\mathcal{G}(\xi) := \bigcup_{p \in \{\sigma, v, 0, 1, -1\}: \xi \in \mathcal{D}_p} \{g_p(\xi)\},$$

$$g_\sigma(\xi) := \begin{bmatrix} \sigma & -\phi & v & -b & q & \tau \end{bmatrix}^\top,$$

$$g_v(\xi) := \begin{bmatrix} \sigma & \frac{k_p}{k_i}\sigma & v & -b & q & \tau \end{bmatrix}^\top,$$

$$g_0(\xi) := \begin{bmatrix} \sigma & \phi & v & b & 0 & \tau \end{bmatrix}^\top,$$

$$g_1(\xi) := \begin{bmatrix} \sigma & \phi & v & b & 1 & 0 \end{bmatrix}^\top,$$

$$g_{-1}(\xi) := \begin{bmatrix} \sigma & \phi & v & b & -1 & 0 \end{bmatrix}^\top. \qquad (43\text{e})$$

The flow and jump sets of $\mathcal{H}_\delta$ are defined as

$$\mathcal{C}_{\text{slip}} := \{\xi \in \Xi : |q| = 1\}$$
$$\mathcal{C}_{\text{stick}} := \{\xi \in \Xi : v = 0, |\phi| \leq F_s, q = 0\}$$
$$\mathcal{D}_\sigma := \{\xi \in \Xi : \sigma = 0, b = 1, |q| = 1\}$$
$$\mathcal{D}_v := \{\xi \in \Xi : v = 0, b = -1, q = 0\}$$
$$\mathcal{D}_0 := \{\xi \in \Xi : v = 0, |q| = 1\}$$
$$\mathcal{D}_1 := \{\xi \in \Xi : v = 0, \phi \geq F_s, b = 1, q = 0, \tau \in [\delta, 2\delta]\}$$
$$\mathcal{D}_{-1} := \{\xi \in \Xi : v = 0, \phi \leq -F_s, b = 1, q = 0, \tau \in [\delta, 2\delta]\}$$
$$(43\text{f})$$

and are visualized in Fig. 8. Based on (43f), we define

$$\mathcal{C} := \mathcal{C}_{\text{slip}} \cup \mathcal{C}_{\text{stick}}, \quad \mathcal{D} := \mathcal{D}_\sigma \cup \mathcal{D}_v \cup \mathcal{D}_0 \cup \mathcal{D}_1 \cup \mathcal{D}_{-1}. \qquad (43\text{g})$$

A hybrid automaton corresponding to $\mathcal{H}_\delta$ is in Fig. 9.

We establish in Proposition 6 that $\mathcal{H}_\delta$ in (43) captures all solutions to the original closed-loop model $\hat{\mathcal{H}}$ in (17) in a semiglobal fashion, which verifies the semiglobal simulation of $\hat{\mathcal{H}}$ by way of $\mathcal{H}_\delta$. Importantly, the next proposition allows extending semiglobally the stability properties of $\mathcal{H}_\delta$ to $\hat{\mathcal{H}}$. For

a hybrid solution ψ, we use, in the proposition, the notation $j(t) := \min_{(t,k) \in \text{dom } \psi} k$. With a slight abuse of notation, we use a unified symbol $j(\cdot)$ because the solution under consideration is always clear from the context.

Proposition 6: Let Assumptions 1 and 2 hold. For each compact set $\mathcal{K}$ and the corresponding $\delta(\mathcal{K}) > 0$ characterized in Proposition 5, for each solution $\hat{\xi} = (\hat{\sigma}, \hat{\phi}, \hat{v}, \hat{b})$ to $\hat{\mathcal{H}}$ with $\hat{\xi}(0,0) = \hat{\xi}_0 \in \mathcal{K}$, there exist q_0, τ_0, and a solution $\xi = (\sigma, \phi, v, b, q, \tau)$ to $\mathcal{H}_{\delta(\mathcal{K})}$ starting at $\xi(0,0) = (\hat{\xi}_0, q_0, \tau_0)$, such that

$$\hat{\sigma}(t, j(t)) = \sigma(t, j(t)), \quad \hat{\phi}(t, j(t)) = \phi(t, j(t))$$
$$\hat{v}(t, j(t)) = v(t, j(t)), \quad \hat{b}(t, j(t)) = b(t, j(t)) \qquad (44)$$

for all $t \geq 0$ such that $\hat{\xi}(t, j(t)) \notin \hat{\mathcal{A}}$.

Proof: First, note that strong forward invariance of $\hat{\mathcal{A}}$ as per Proposition 3(1) implies that, for any solution $\hat{\xi}$, property $\hat{\xi}(t, j(t)) \notin \hat{\mathcal{A}}$ implies $\hat{\xi}(s, j(s)) \notin \hat{\mathcal{A}}$ for all $s \leq t$. Hence, the semiglobal dwell time conclusions of Proposition 5 apply for the time instants t considered in (44).

It is apparent that: 1) the timer τ does not affect the flow or jump maps of components (σ, ϕ, v, b, q) in (43d) and (43e) and 2) it may inhibit jumps *only* from $\mathcal{D}_1$ or $\mathcal{D}_{-1}$, see (43g) and the graphical representation in Fig. 9. Due to this reason, we begin by selecting $\tau_0 = \delta(\mathcal{K})$ so that no jumps are inhibited at $(0,0)$. In fact, the conditions in the sets $\mathcal{D}_1$ and $\mathcal{D}_{-1}$ show them to be suitable liftings to higher dimensional spaces (involving the extra variables q and τ) of, respectively, the sets $\hat{\mathcal{S}}_1$ and $\hat{\mathcal{S}}_{-1}$ defined in (36). As a consequence, we may prove the simulation property (44) without focusing on the timer τ because the fact that $\hat{\xi} = (\hat{\sigma}, \hat{\phi}, \hat{v}, \hat{b})$ and the components (σ, ϕ, v, b) of a solution ξ coincide over a time interval implies, by the semiglobal dwell time of $\hat{\xi}$ in Proposition 5, that the condition on τ enforced in $\mathcal{D}_1$ and $\mathcal{D}_{-1}$ is always satisfied since the velocity $\hat{v}$ will not change its sign for a time interval of length at least $\delta(\mathcal{K})$. This is done in the next lemma, whose proof amounts to checking all the possible (nonunique) evolutions of $\hat{\mathcal{H}}$ and of $\mathcal{H}_{\delta(\mathcal{K})}$, and is here omitted due to space constraints but can be found in [12].

Lemma 4: Under Assumptions 1 and 2, for each solution $\hat{\xi} = (\hat{\sigma}, \hat{\phi}, \hat{v}, \hat{b})$ to $\hat{\mathcal{H}}$ with $\hat{\xi}(0,0) = \hat{\xi}_0 \in \mathcal{K}$, there exists q_0 such that some solution ξ to $\mathcal{H}_{\delta(\mathcal{K})}$ with $\mathcal{D}_1$ and $\mathcal{D}_{-1}$ replaced by

$$\bar{\mathcal{D}}_1 := \{\xi \in \Xi : v = 0, \phi \geq F_s, b = 1, q = 0\} \qquad (45\text{a})$$
$$\bar{\mathcal{D}}_{-1} := \{\xi \in \Xi : v = 0, \phi \leq -F_s, b = 1, q = 0\} \qquad (45\text{b})$$

(namely, without any τ-induced jump inhibition), starting at $\xi(0,0) = (\hat{\xi}_0, q_0, \delta(\mathcal{K}))$ satisfies (44) for all $t \geq 0$ such that $\hat{\xi}(t, j(t)) \notin \hat{\mathcal{A}}$.

The solution ξ characterized in Lemma 4 never reaches $\bar{\mathcal{D}}_1$ or $\bar{\mathcal{D}}_{-1}$ with $\tau < \delta(\mathcal{K})$; otherwise, the solution $\hat{\xi}$ would belong to $\hat{\mathcal{S}}_1$ or $\hat{\mathcal{S}}_{-1}$ in (36), contradicting Proposition 5. Thus, ξ is also a solution to $\mathcal{H}_{\delta(\mathcal{K})}$, and this completes the proof. $\square$

VI. STABILITY ANALYSIS

For the simulation model $\mathcal{H}_\delta$ of Section V-C, we construct in Section VI-A a weak Lyapunov function V. Based on V, GAS of $\mathcal{H}_\delta$ is proven in Section VI-B.

Finally, in Section VI-C, the semiglobal simulation result of Proposition 6 is used to prove Theorem 1.

A. Lipschitz Lyapunov Function for the Simulation Model

To prove suitable stability properties of $\mathcal{H}_\delta$ in (43), we introduce the following lifting of the attractor $\hat{\mathcal{A}}$ in (18) as:

$$\mathcal{A} := \{\xi \in \Xi : \sigma = v = 0, \phi \in F_s \operatorname{Sign}(bq)\} \tag{46}$$

where the extra variables q and τ can be selected arbitrarily within the set Ξ.

The advantage of introducing $\mathcal{H}_\delta$ resides in the next locally Lipschitz Lyapunov function

$$V(\xi) := \begin{bmatrix} \sigma \\ v \end{bmatrix}^\top \begin{bmatrix} \dfrac{k_d}{k_i} & -1 \\ -1 & k_p \end{bmatrix} \begin{bmatrix} \sigma \\ v \end{bmatrix} + |q|(\phi - bqF_s)^2$$
$$+ (1 - |q|)\mathrm{dz}_{F_s}^2(\phi) + 2\dfrac{k_p}{k_i}F_s\big(bq\sigma + (1 - |q|)|\sigma|\big) \tag{47}$$

where the first three terms can be seen as a smooth version of the discontinuous Lyapunov-like function (23) and the last nonsmooth nonnegative term ensures a desirable nonincrease property along dynamics (43). To deal with the nonsmooth (but Lipschitz) expression $|\sigma|$ in the last term, we use the Clarke generalized gradient $\partial V(y)$ of V at y (see [20, Ch. 2]).

The next proposition establishes useful properties required of a hybrid Lyapunov function, that is, positive definiteness with respect to $\mathcal{A}$ in $\mathcal{C} \cup \mathcal{D}$ (this property being also called *copositivity with respect to* $\mathcal{C} \cup \mathcal{D}$ in the research area surveyed in [18]) and radial unboundedness, nonincrease along flow in $\mathcal{C}$, and nonincrease across jumps from $\mathcal{D}$. These properties establish what we could not prove in Lemma 2 for function W in (23), where (27) was only guaranteed when flowing with $\hat{b} = -1$.

Proposition 7: Under Assumptions 1 and 2, the Lyapunov function V in (47) satisfies the next properties along dynamics (43).
1) V is positive definite with respect to $\mathcal{A}$ in $\mathcal{C} \cup \mathcal{D}$ and radially unbounded relative to $\mathcal{C} \cup \mathcal{D}$.
2) With $c_3 > 0$ in (25), we have

$$V^\circ(\xi) := \max_{v \in \partial V(\xi)} \langle v, \mathcal{F}(\xi) \rangle \leq -c_3 v^2 \leq 0 \quad \forall \xi \in \mathcal{C}. \tag{48}$$

3) For each $p \in \{\sigma, v, 1, -1, 0\}$, we have

$$\Delta V_p(\xi) := V(g_p(\xi)) - V(\xi) \leq 0 \quad \forall \xi \in \mathcal{D}_p. \tag{49}$$

Proof: We prove the proposition item by item.

Item (1): Positive definiteness with respect to $\mathcal{A}$ in $\mathcal{C} \cup \mathcal{D}$ follows by verifying that for each $\xi \in \mathcal{C} \cup \mathcal{D}$, $V(\xi) \geq 0$ and $V(\xi) = 0$ if and only if $\xi \in \mathcal{A}$. To see this, for each $\xi \in \mathcal{C} \cup \mathcal{D}$, V is a sum of nonnegative terms in (47) since the 2×2 matrix is positive definite from Assumption 2, and $bq\sigma \geq 0$ in $\mathcal{C} \cup \mathcal{D}$, see Ξ in (43a). Moreover, for each $\xi \in \mathcal{C} \cup \mathcal{D}$, $V(\xi) = 0$ if and only if $\xi \in \mathcal{A}$ because $\xi \in \mathcal{A}$ implies that $V(\xi) = |q|(\phi - bqF_s)^2 = 0$, and $V(\xi) = 0$ implies that all the nonnegative terms of the sum in (47) must be zero: hence, $\sigma = v = 0$; for $|q| = 1$, $\phi = bqF_s$; for $q = 0$, $\phi \in [-F_s, F_s]$, and the last two cases imply together $\phi \in F_s \operatorname{Sign}(bq)$. Radial unboundedness must be checked only in the σ, v, and ϕ components because b, q, and τ are bounded

in $\mathcal{C} \cup \mathcal{D} \subset \Xi$. To this end, nonnegativity of the last two terms in (47) and positive definiteness of $\begin{bmatrix} (k_d/k_i) & -1 \\ -1 & k_p \end{bmatrix}$ (from Assumption 2) show the result.

Item (2): For the derivation of V°, we use $(d/d\phi)$ $(\mathrm{dz}_{F_s}^2(\phi)) = 2\mathrm{dz}_{F_s}(\phi)$, and $\partial(|\sigma|) = \operatorname{Sign}(\sigma)$. From (43d)

$$V^\circ(\xi)$$
$$= 2\dfrac{k_d}{k_i}\sigma\dot\sigma - 2v\dot\sigma - 2\sigma\dot v + 2k_p v\dot v + 2|q|(\phi - bqF_s)\dot\phi$$
$$+ 2(1 - |q|)\mathrm{dz}_{F_s}(\phi)\dot\phi + 2\dfrac{k_p}{k_i}F_s bq\dot\sigma$$
$$+ \max_{\varsigma \in \operatorname{Sign}(\sigma)}\left(2\dfrac{k_p}{k_i}F_s(1 - |q|)\varsigma\dot\sigma\right)$$
$$= 2\dfrac{k_d}{k_i}\sigma(-k_i v) - 2v(-k_i v) - 2\sigma(-k_d v + |q|\,\phi - q(F_s$$
$$- |f(v)|)) + 2k_p v(-k_d v + |q|\,\phi - q(F_s - |f(v)|))$$
$$+ 2|q|(\phi - bqF_s)(\sigma - k_p v) + 2(1 - |q|)\mathrm{dz}_{F_s}(\phi)(\sigma - k_p v)$$
$$+ 2\dfrac{k_p}{k_i}F_s bq(-k_i v) + \max_{\varsigma \in \operatorname{Sign}(\sigma)}\left(2\dfrac{k_p}{k_i}F_s(1 - |q|)\varsigma(-k_i v)\right).$$

In this expression, the deadzone term is zero because $|q| = 1$ in $\mathcal{C}_{\text{slip}}$, and $q = 0$ and $|\phi| \leq F_s$ in $\mathcal{C}_{\text{stick}}$; similarly, the term in the maximum is zero because $|q| = 1$ in $\mathcal{C}_{\text{slip}}$, and $q = 0$ and $v = 0$ in $\mathcal{C}_{\text{stick}}$. Since $|q|q = q$ for $\xi \in \Xi$, some computations yield

$$V^\circ(\xi) = -2\ c_3\ v^2 + 2q\sigma(F_s - |f(v)|) - 2F_s bq\sigma$$
$$-2k_p qv(F_s - |f(v)|)$$
$$\leq -2\ c_3\ v^2 + 2q\sigma(F_s - |f(v)|)$$
$$-2F_s bq\sigma \leq -2\ c_3\ v^2 \leq 0$$

where the first inequality follows from $qv \geq 0$ in $\mathcal{C}$ and $F_s - |f(v)| \geq 0$ for all v by Assumption 1(1), and the second inequality follows from $bq\sigma \geq 0$ in $\mathcal{C}$ and $2q\sigma(F_s - |f(v)|) - 2F_s bq\sigma \leq 2|q||\sigma|(F_s - |f(v)|) - 2\ F_s|q||\sigma| = -2|q||\sigma||f(v)| \leq 0$.

Item (3): In (49), we address separately each p corresponding to a jump from $\mathcal{D}_p$ with jump map g_p.

Jump $p = \sigma$: For each $\xi \in \mathcal{D}_\sigma$, $|q| = |q^+| = 1$ and $\sigma = 0$, so

$$\Delta V_\sigma(\xi) = (\phi^+ - b^+ qF_s)^2 - (\phi - bqF_s)^2$$
$$= (-\phi + bqF_s)^2 - (\phi - bqF_s)^2 = 0.$$

Jump $p = v$: For each $\xi \in \mathcal{D}_v$, $q = q^+ = 0$, so

$$\Delta V_v(\xi) = \mathrm{dz}_{F_s}^2(\phi^+) - \mathrm{dz}_{F_s}^2(\phi) = \mathrm{dz}_{F_s}^2(|\phi^+|) - \mathrm{dz}_{F_s}^2(|\phi|) \leq 0$$

because $|\phi^+| = (k_p/k_i)|\sigma| \leq |\phi|$ from constraint $\sigma\phi \geq (k_p/k_i)\sigma^2 \geq 0$ in $\mathcal{D}_v$, which is equivalent to $|\sigma||\phi| \geq (k_p/k_i)|\sigma|^2$.

Jump $p \in \{1, -1\}$: For each $\xi \in \mathcal{D}_{-1}$ or $\xi \in \mathcal{D}_1$, $b = b^+ = 1$, $q = 0$, and $|q^+| = 1$, so

$$\Delta V_i(\xi) = (\phi - bq^+ F_s)^2 - \mathrm{dz}_{F_s}^2(\phi) + 2\dfrac{k_p}{k_i}F_s bq^+\sigma - 2\dfrac{k_p}{k_i}F_s|\sigma|$$
$$\leq (\phi - q^+ F_s)^2 - \mathrm{dz}_{F_s}^2(\phi) = 0$$

where the inequality holds since $bq^+\sigma \leq |\sigma|$ and the last equality holds since $q^+\phi \geq F_s$.

Jump $p = 0$: For each $\xi \in \mathcal{D}_0$, $|q| = 1$ and $q^+ = 0$, so

$$\Delta V_0(\xi) = \mathrm{dz}_{F_s}^2(\phi) - (\phi - bqF_s)^2 + 2\frac{k_p}{k_i}F_s|\sigma| - 2\frac{k_p}{k_i}F_s bq\sigma$$

$$= \mathrm{dz}_{F_s}^2(\phi) - (\phi - bqF_s)^2 \le 0$$

where the last equality holds since $bq\sigma = |\sigma|$ (by $bq\sigma \ge 0$, $|b| = 1$, and $|q| = 1$ in $\mathcal{D}_0$) and the inequality holds since $bq \in \{-1, 1\}$.   □

B. Global Asymptotic Stability of the Simulation Model

Proposition 7 shows that function V in (47) is a weak Lyapunov function certifying stability of $\mathcal{A}$ in (46) for $\mathcal{H}_\delta$. To establish global attractivity (thus, global asymptotic stability), we exploit the hybrid invariance principle in [42, Th. 1] in the next proposition.

Proposition 8: Under Assumptions 1 and 2, for each $\delta > 0$, the set $\mathcal{A}$ in (46) is GAS for $\mathcal{H}_\delta$ in (43).

Proof: The proof is based on [42, Th. 1]. The set $\mathcal{A}$ in (46) is compact, and $\mathcal{H}_\delta$ in (43) satisfies the hybrid basic conditions in [25, Assumption 6.5]. We check the other assumptions of [42, Th. 1] in the following.

1) $\mathcal{G}(\mathcal{D} \cap \mathcal{A}) \subset \mathcal{A}$ *for $\mathcal{G}$ in (43b):* Indeed, $g_\sigma(\mathcal{D}_\sigma \cap \mathcal{A}) \subset g_\sigma(\mathcal{A}) \subset \mathcal{A}$, $g_v(\mathcal{D}_v \cap \mathcal{A}) \subset \mathcal{A}$, $g_0(\mathcal{D}_0 \cap \mathcal{A}) \subset g_0(\mathcal{A}) \subset \mathcal{A}$, $g_1(\mathcal{D}_1 \cap \mathcal{A}) \subset \mathcal{A}$, and $g_{-1}(\mathcal{D}_{-1} \cap \mathcal{A}) \subset \mathcal{A}$.

2) *Conditions on V:* The Lyapunov function V satisfies $\mathcal{C} \cup \mathcal{D} \subset \mathrm{dom}\, V$, is continuous in $\mathcal{C} \cup \mathcal{D}$ and locally Lipschitz near each point in $\mathcal{C}$, and is positive definite with respect to $\mathcal{A}$ in $\mathcal{C} \cup \mathcal{D}$ and radially unbounded relative to $\mathcal{C} \cup \mathcal{D}$ by Proposition 7(1). The Lyapunov nonincrease conditions have been established in Proposition 7(2-3).

3) *No Complete Solution Keeps V Constant and Nonzero:* We preliminarily show that the dwell time enforced by the timer τ in $\mathcal{H}_\delta$ and the logical variables imply that complete solutions exhibit an infinite amount of flow. If not, we could remove from the automaton of Fig. 9 the jumps from $\mathcal{D}_1$ or $\mathcal{D}_{-1}$ (which are only enabled if $\tau \ge \delta$). The remaining jumps are those in Fig. 10, revealing that, when $\tau < \delta$, after at most two jumps, it must hold that $q = 0$. From $q = 0$, the only possible jump is from $\mathcal{D}_v$ (where $b = -1$), which maps to $b = 1$, so that at most one jump from $\mathcal{D}_v$ is possible. In summary, at most three jumps can happen when $\tau < \delta$, and the solution would not be complete. This proves that all complete solutions exhibit an infinite amount of flow.

Now suppose, by contradiction, that there exists a complete solution ξ_{bad} to $\mathcal{H}_\delta$ that keeps V constant and nonzero. Being complete, this solution exhibits an infinite amount of flow, which should happen outside $\mathcal{A}$ (otherwise, V would be zero). Moreover, ξ_{bad} must start with a zero initial velocity v, which should remain zero all along with the solution, because v remains constant across any possible jump, and any flowing solution from $v \ne 0$ will cause a decrease of V from item (2) of Proposition 7.

Such a flowing solution with $v \equiv 0$ cannot flow in $\mathcal{C}_{\mathrm{slip}} \backslash \mathcal{A}$. Indeed, $f(v) = L_2 v$ for all $|v| \le \varepsilon_v$ by
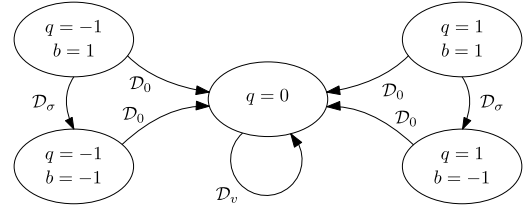

Fig. 10.   Auxiliary version of the hybrid automaton in Fig. 9 used in the proof of Proposition 8.

Assumption 1(4). We have then from (43d) that the first three components of $\mathcal{F}$ are

$$\text{for } q = 1 : \begin{bmatrix} -k_i v \\ \sigma - k_p v \\ -k_d v + \phi - F_s + L_2 v \end{bmatrix} =: A_{L_2}\begin{bmatrix} \sigma \\ \phi - F_s \\ v \end{bmatrix},$$

$$\text{for } q = -1 : \begin{bmatrix} -k_i v \\ \sigma - k_p v \\ -k_d v + \phi + F_s + L_2 v \end{bmatrix} =: A_{L_2}\begin{bmatrix} \sigma \\ \phi + F_s \\ v \end{bmatrix}$$

with $A_{L_2} := \begin{bmatrix} 0 & 0 & -k_i \\ 1 & 0 & -k_p \\ 0 & 1 & -k_d + L_2 \end{bmatrix}$. Since the pair $([\,0\;0\;1\,], A_{L_2})$ is observable, the only solutions (σ, ϕ, v) compatible with $v \equiv 0$ are constant and correspond to the points where $v = 0$ and $\begin{bmatrix} q \\ b \\ \sigma \\ \phi \end{bmatrix} = \begin{bmatrix} 1 \\ 1 \\ 0 \\ F_s \end{bmatrix}$ and $\begin{bmatrix} q \\ b \\ \sigma \\ \phi \end{bmatrix} = \begin{bmatrix} -1 \\ 1 \\ 0 \\ -F_s \end{bmatrix}$, where the value of b is imposed by the constraint $bq\phi \ge 0$ in $\mathcal{C}_{\mathrm{slip}}$. By (46), both points belong to $\mathcal{A}$, so ξ_{bad} cannot evolve there.

We conclude by showing that ξ_{bad} cannot flow indefinitely in $\mathcal{C}_{\mathrm{stick}} \backslash \mathcal{A}$. Indeed, the first three components of $\mathcal{F}$ in (43d) are $(0, \sigma, 0)$, with σ being nonzero (otherwise, ξ_{bad} would be in $\mathcal{A}$). With such indefinite flowing, ϕ would grow unbounded and this contradicts $|\phi| \le F_s$ (required in $\mathcal{C}_{\mathrm{stick}} \backslash \mathcal{A}$). In particular, any such ξ_{bad} must eventually reach a point, where $(v, \sigma, \phi, b) = (0, \sigma, \mathrm{sign}(\sigma)F_s, 1)$ (possibly after a jump from $\mathcal{D}_v$), from where it must jump from $\mathcal{D}_1$ or $\mathcal{D}_{-1}$ to a point where $|q^+| = 1$, $\sigma^+ = \sigma$ is nonzero, and $b^+ = 1$. Any subsequent flow (which must happen because an infinite amount of flow occurs) must occur in $\mathcal{C}_{\mathrm{slip}} \backslash \mathcal{A}$ and is ruled out by the previous analysis. Hence, the proof is complete.   □

C. Proof of Theorem 1

We are now able to prove Theorem 1 because the semiglobal similarity properties of Proposition 6 allow extending the stability results of Proposition 8 to system $\hat{\mathcal{H}}$ in (17), provided that solutions are bounded as per Proposition 4.

First, define

$$\hat{\mathcal{A}}_6 := \big\{ (\hat{\sigma}, \hat{\phi}, \hat{v}, \hat{b}, q, \tau) : \hat{\sigma} = \hat{v} = 0, |\hat{\phi}| \le F_s,$$
$$\hat{b} \in \{-1, 1\}, q \in \{-1, 0, 1\}, \tau \in [0, 2\delta] \big\},$$

which extends $\hat{\mathcal{A}} \subset \mathbb{R}^4$ in (18) to the new directions q and τ so that $\hat{\mathcal{A}}_6 \subset \mathbb{R}^6$. It holds that $\hat{\mathcal{A}}_6 \supset \mathcal{A}$ with $\mathcal{A}$ in (46). Then, for each $\xi = (\hat{\xi}, q, \tau) \in \Xi$

$$|\xi|_{\mathcal{A}} := \inf_{y \in \mathcal{A}} |\xi - y| \ge \inf_{y \in \hat{\mathcal{A}}_6} |\xi - y|$$

$$= \inf_{y \in \hat{\mathcal{A}}_6} |(\hat{\xi}, q, \tau) - y| = |\hat{\xi}|_{\hat{\mathcal{A}}}. \qquad (50)$$

We need to show stability and global attractivity of $\hat{\mathcal{A}}$, where the latter entails by [25, Definition 7.1] that, for each solution $\hat{\hat{\xi}}$ to $\hat{\mathcal{H}}$, $\hat{\hat{\xi}}$ is bounded and satisfies

$$\lim_{t+j\to\infty} \left| \hat{\hat{\xi}}(t,j) \right|_{\hat{\mathcal{A}}} = 0 \tag{51}$$

since maximal solutions are complete by Proposition 1. Boundedness of solutions is guaranteed by Proposition 4. Proposition 6 guarantees that, for each compact set $\mathcal{K}$ and the corresponding $\delta(\mathcal{K}) > 0$, each solution $\hat{\hat{\xi}}$ to $\hat{\mathcal{H}}$ with $\hat{\hat{\xi}}(0,0) \in \mathcal{K}$ coincides with the $(\sigma, \phi, \upsilon, b)$ components of some solution ξ to $\mathcal{H}_{\delta(\mathcal{K})}$ for all $t \geq 0$ such that $\hat{\hat{\xi}}(t, j(t)) \notin \hat{\mathcal{A}}$, i.e., it holds from (44) that $\xi(t, j(t)) = (\hat{\hat{\xi}}(t, j(t)), q(t, j(t)), \tau(t, j(t)))$ for all $t \geq 0$ such that $\hat{\hat{\xi}}(t, j(t)) \notin \hat{\mathcal{A}}$. Then, (50) implies that

$$\left| \xi(t, j(t)) \right|_{\mathcal{A}} \geq \left| \hat{\hat{\xi}}(t, j(t)) \right|_{\hat{\mathcal{A}}} \tag{52}$$

for all $t \geq 0$ such that $\hat{\hat{\xi}}(t, j(t)) \notin \hat{\mathcal{A}}$. If there exists $t' \geq 0$ such that $\hat{\hat{\xi}}(t', j(t')) \in \hat{\mathcal{A}}$, then (51) is proven by Proposition 3(1). If instead $\hat{\hat{\xi}}(t, j(t)) \notin \hat{\mathcal{A}}$ for all t in the domain of $\hat{\hat{\xi}}$, then $\sup_t \hat{\hat{\xi}} = +\infty$ by Proposition 3(2), and then, $\sup_t \xi = +\infty$ as well by (44). Moreover, Proposition 8 implies that $\lim_{t\to\infty} \left| \xi(t, j(t)) \right|_{\mathcal{A}} = 0$, which with (52) proves (51) and global attractivity of $\hat{\mathcal{A}}$.

Since $\mathcal{A}$ is compact and both $\mathcal{H}_\delta$ and $\hat{\mathcal{H}}$ satisfy the hybrid basic conditions [25, Assumption 6.5], the global asymptotic stability of $\mathcal{A}$ for $\mathcal{H}_\delta$ in Proposition 8 implies uniform global stability and uniform global attractivity by [25, Th. 7.12]. Hence, $\hat{\mathcal{A}}$ is uniformly globally attractive. Since $\hat{\mathcal{A}}$ is also strongly forward invariant by Proposition 3(1), then $\hat{\mathcal{A}}$ is stable by [25, Proposition 7.5], which, together with its global attractivity, implies its global asymptotic stability.

VII. CONCLUSION

We proposed a novel reset integrator control strategy for motion systems with unknown Coulomb and velocity-dependent friction (including the Stribeck effect) that achieves global asymptotic stability of the setpoint. The working principle and effectiveness of the controller are experimentally demonstrated in a case study on a high-precision positioning application. Interesting future research directions include addressing more general nonsmooth multibody mechanical systems with several contact points with friction, in addition to investigating the use of set-valued chattering-free sliding mode control [3], thus obtaining finite-time stabilization and possibly exploiting the tools given in [4], for motion control applications.

REFERENCES

[1] W. H. T. M. Aangenent, G. Witvoet, W. P. M. H. Heemels, M. J. G. van de Molengraft, and M. Steinbuch, "Performance analysis of reset control systems," *Int. J. Robust Nonlinear Control*, vol. 20, no. 11, pp. 1213–1233, Jul. 2010.

[2] V. Acary and B. Brogliato, *Numerical Methods for Nonsmooth Dynamical Systems*. Berlin, Germany: Springer, 2008.

[3] V. Acary and B. Brogliato, "Implicit Euler numerical scheme and chattering-free implementation of sliding mode systems," *Syst. Control Lett.*, vol. 59, no. 5, pp. 284–293, May 2010.

[4] J. Alvarez, I. Orlov, and L. Acho, "An invariance principle for discontinuous dynamic systems with application to a Coulomb friction oscillator," *J. Dyn. Syst., Meas., Control*, vol. 122, no. 4, pp. 687–690, Dec. 2000.

[5] A. Amthor, S. Zschaeck, and C. Ament, "High precision position control using an adaptive friction compensation approach," *IEEE Trans. Autom. Control*, vol. 55, no. 1, pp. 274–278, Jan. 2010.

[6] B. Armstrong and B. Amin, "PID control in the presence of static friction: A comparison of algebraic and describing function analysis," *Automatica*, vol. 32, no. 5, pp. 679–692, May 1996.

[7] B. Armstrong-Hélouvry, P. Dupont, and C. Canudas De Wit, "A survey of models, analysis tools and compensation methods for the control of machines with friction," *Automatica*, vol. 30, no. 7, pp. 1083–1138, Jul. 1994.

[8] J.-P. Aubin, J. Lygeros, M. Quincampoix, S. Sastry, and N. Seube, "Impulse differential inclusions: A viability approach to hybrid systems," *IEEE Trans. Autom. Control*, vol. 47, no. 1, pp. 2–20, 2002.

[9] A. Baños and A. Barreiro, *Reset Control System*. London, U.K.: Springer, 2011.

[10] G. Bartolini and E. Punta, "Chattering elimination with second-order sliding modes robust to Coulomb friction," *J. Dyn. Syst., Meas., Control*, vol. 122, no. 4, pp. 679–686, Dec. 2000.

[11] R. Beerens, A. Bisoffi, L. Zaccarian, W. P. M. H. Heemels, H. Nijmeijer, and N. van de Wouw, "Reset integral control for improved settling of PID-based motion systems with friction," *Automatica*, vol. 107, pp. 483–492, Sep. 2019.

[12] R. Beerens, A. Bisoffi, L. Zaccarian, H. Nijmeijer, W. P. M. H. Heemels, and N. van de Wouw. (Jan. 2020). *Reset PID Design for Motion Systems With Stribeck Friction*. [Online]. Available: https://hal.archives-ouvertes.fr/hal-02454405

[13] O. Beker, C. V. Hollot, and Y. Chait, "Plant with integrator: An example of reset control overcoming limitations of linear feedback," *IEEE Trans. Autom. Control*, vol. 46, no. 11, pp. 1797–1799, Dec. 2001.

[14] A. Bisoffi, R. Beerens, L. Zaccarian, W. P. M. H. Heemels, H. Nijmeijer, and N. van de Wouw, "Hybrid model formulation and stability analysis of a PID-controlled motion system with Coulomb friction," *IFAC-PapersOnLine*, vol. 52, pp. 84–89, Jan. 2019.

[15] A. Bisoffi, M. Da Lio, A. R. Teel, and L. Zaccarian, "Global asymptotic stability of a PID control system with Coulomb friction," *IEEE Trans. Autom. Control*, vol. 63, no. 8, pp. 2654–2661, Aug. 2018.

[16] F. Blanchini and S. Miani, *Set-Theoretic Methods Control*. Cham, Switzerland: Springer, 2008.

[17] B. Brogliato and A. Tanwani, "Dynamical systems coupled with monotone set-valued operators: Formalisms, applications, well-posedness, and stability," *SIAM Rev.*, vol. 62, no. 1, pp. 3–129, Jan. 2020.

[18] M. K. Çamlıbel and J. M. Schumacher, "Copositive Lyapunov functions," in *Unsolved Problems in Mathematical Systems and Control Theory*, V. D. Blondel and A. Megretski, Eds. Princeton, NJ, USA: Princeton University Press, 2004, pp. 189–193.

[19] W. Chen, K. Kong, and M. Tomizuka, "Dual-stage adaptive friction compensation for precise load side position tracking of indirect drive mechanisms," *IEEE Trans. Control Syst. Technol.*, vol. 23, no. 1, pp. 164–175, Jan. 2015.

[20] F. H. Clarke, *Optimization Nonsmooth Analysis*. Philadelphia, PA, USA: SIAM, 1990.

[21] J. C. Clegg, "A nonlinear integrator for servomechanisms," *Trans. Amer. Inst. Electr. Eng., II, Appl. Ind.*, vol. 77, no. 1, pp. 41–42, 1958.

[22] J. C. A. de Bruin, A. Doris, N. van de Wouw, W. P. M. H. Heemels, and H. Nijmeijer, "Control of mechanical motion systems with non-collocation of actuation and friction: A Popov criterion approach for input-to-state stability and set-valued nonlinearities," *Automatica*, vol. 45, no. 2, pp. 405–415, Feb. 2009.

[23] D. A. Deenen, M. F. Heertjes, W. P. M. H. Heemels, and H. Nijmeijer, "Hybrid integrator design for enhanced tracking in motion control," *Proc. Amer. Control Conf.*, 2017, pp. 2863–2868.

[24] L. Freidovich, A. Robertsson, A. Shiriaev, and R. Johansson, "LuGre-model-based friction compensation," *IEEE Trans. Control Syst. Technol.*, vol. 18, no. 1, pp. 194–200, Jan. 2010.

[25] R. Goebel, R. G. Sanfelice, and A. R. Teel, *Hybrid Dynamical Systems*. Princeton, NJ, USA: Princeton Univ. Press, 2012.

[26] E. Haghverdi, P. Tabuada, and G. J. Pappas, "Bisimulation relations for dynamical, control, and hybrid systems," *Theor. Comput. Sci.*, vol. 342, nos. 2–3, pp. 229–261, Sep. 2005.

[27] R. H. A. Hensen, M. J. G. van de Molengraft, and M. Steinbuch, "Friction induced hunting limit cycles: A comparison between the LuGre and switch friction model," *Automatica*, vol. 39, no. 12, pp. 2131–2137, Dec. 2003.

[28] I. Horowitz and P. Rosenbaum, "Non-linear design for cost of feedback reduction in systems with large parameter uncertainty," *Int. J. Control*, vol. 21, no. 6, pp. 977–1001, Jun. 1975.

[29] L. Iannelli, K. H. Johansson, U. T. Jönsson, and F. Vasca, "Averaging of nonsmooth systems using dither," *Automatica*, vol. 42, no. 4, pp. 669–676, Apr. 2006.

[30] V. Lampaert, J. Swevers, and F. Al-Bender, "Modification of the Leuven integrated friction model structure," *IEEE Trans. Autom. Control*, vol. 47, no. 4, pp. 683–687, Apr. 2002.

[31] C. Makkar, G. Hu, W. G. Sawyer, and W. E. Dixon, "Lyapunov-based tracking control in the presence of uncertain nonlinear parameterizable friction," *IEEE Trans. Autom. Control*, vol. 52, no. 10, pp. 1988–1994, Oct. 2007.

[32] D. Nešić, A. R. Teel, and L. Zaccarian, "Stability and performance of SISO control systems with first-order reset elements," *IEEE Trans. Autom. Control*, vol. 56, no. 11, pp. 2567–2582, Nov. 2011.

[33] D. Nešić, L. Zaccarian, and A. R. Teel, "Stability properties of reset systems," *Automatica*, vol. 44, no. 8, pp. 2019–2026, Aug. 2008.

[34] Y. Orlov, L. Aguilar, and J. C. Cadiou, "Switched chattering control vs. backlash/friction phenomena in electrical servo-motors," *Int. J. Control*, vol. 76, nos. 9–10, pp. 959–967, Jan. 2003.

[35] Y. Orlov, R. Santiesteban, and L. T. Aguilar, "Impulsive control of a mechanical oscillator with friction," in *Proc. Amer. Control Conf.*, 2009, pp. 3494–3499.

[36] P. Prabhakar, G. Dullerud, and M. Viswanathan, "Stability preserving simulations and bisimulations for hybrid systems," *IEEE Trans. Autom. Control*, vol. 60, no. 12, pp. 3210–3225, Dec. 2015.

[37] C. Prieur, I. Queinnec, S. Tarbouriech, and L. Zaccarian, "Analysis and synthesis of reset control systems," *Found. Trends Syst. Control*, vol. 6, nos. 2–3, pp. 117–338, 2019.

[38] D. Putra, H. Nijmeijer, and N. van de Wouw, "Analysis of undercompensation and overcompensation of friction in 1DOF mechanical systems," *Automatica*, vol. 43, no. 8, pp. 1387–1394, Aug. 2007.

[39] M. Ruderman and M. Iwasaki, "Analysis of linear feedback position control in presence of presliding friction," *IEEJ J. Ind. Appl.*, vol. 5, no. 2, pp. 61–68, Mar. 2016.

[40] M. Ruderman and M. Iwasaki, "Observer of nonlinear friction dynamics for motion control," *IEEE Trans. Ind. Electron.*, vol. 62, no. 9, pp. 5941–5949, Sep. 2015.

[41] M. M. Seron, J. H. Braslavsky, and G. C. Goodwin, *Fundamental Limitations in Filtering and Control*. Berlin, Germany: Springer, 1997.

[42] A. Seuret, C. Prieur, S. Tarbouriech, A. R. Teel, and L. Zaccarian, "A nonsmooth hybrid invariance principle applied to robust event-triggered design," *IEEE Trans. Autom. Control*, vol. 64, no. 5, pp. 2061–2068, May 2019.

[43] E. D. Sontag, "An algebraic approach to bounded controllability of linear systems," *Int. J. Control*, vol. 39, no. 1, pp. 181–188, Jan. 1984.

[44] R. Stribeck, "Die wesentlichen Eigenschaften der Gleit- und Rollenlager," *Zeitschrift des Vereines Deutscher Ingenieure*, vol. 46 nos. 38–39, pp. 1342–1348, 1902.

[45] *Thermo Fisher Scientific*. Accessed: Mar. 9, 2021. [Online]. Available: https://www.fei.com/products/

[46] N. van de Wouw and R. I. Leine, "Robust impulsive control of motion systems with uncertain friction," *Int. J. Robust Nonlinear Control*, vol. 22, no. 4, pp. 369–397, Mar. 2012.

[47] S. J. A. M. van den Eijnden, M. F. Heertjes, W. P. M. H. Heemels, and H. Nijmeijer, "Hybrid integrator-gain systems: A remedy for overshoot limitations in linear control?" *IEEE Contr. Syst. Lett.*, vol. 4, no. 4, pp. 1042–1047, Jun. 2020.

[48] A. van der Schaft, "Equivalence of dynamical systems by bisimulation," *IEEE Trans. Autom. Control*, vol. 49, no. 12, pp. 2160–2172, Dec. 2004.

[49] S. J. L. M. van Loon, K. G. J. Gruntjens, M. F. Heertjes, N. van de Wouw, and W. P. M. H. Heemels, "Frequency-domain tools for stability analysis of reset control systems," *Automatica*, vol. 82, pp. 101–108, Aug. 2017.

[50] S. J. L. M. van Loon, B. G. B. Hunnekens, W. P. M. H. Heemels, N. van de Wouw, and H. Nijmeijer, "Split-path nonlinear integral control for transient performance improvement," *Automatica*, vol. 66, pp. 262–270, Apr. 2016.

Andrea Bisoffi (Member, IEEE) received the M.Sc. degree in automatic control engineering from the Politecnico di Milano, Milan, Italy, in 2013, and the Ph.D. degree in mechatronics from the University of Trento, Trento, Italy, in 2017.

He was a Post-Doctoral Researcher at the KTH Royal Institute of Technology, Stockholm, Sweden, from 2017 to 2019, and is currently one at the University of Groningen, Groningen, The Netherlands. His research interest includes hybrid and nonlinear control systems, with applications to mechanical and robotic systems.

Luca Zaccarian (Fellow, IEEE) received the Ph.D. degree from the University of Roma Tor Vergata, Rome, Italy, in 2000.

He became an Assistant and then an Associate Professor with the University of Roma Tor Vergata. Since 2011, he has been Directeur de Recherche at the LAAS-CNRS, Toulouse, France, and since 2013, he has been holding a part-time professorship at the University of Trento, Trento, Italy. His main research interests include analysis and design of nonlinear and hybrid control systems, and modeling and control of mechatronic systems.

Dr. Zaccarian was a recipient of the 2001 O. Hugo Schuck Best Paper Award given by the American Automatic Control Council.

Henk Nijmeijer (Life Fellow, IEEE) was born in 1955.

He is a Full Professor at the Eindhoven University of Technology, Eindhoven, The Netherlands, and chairs the Dynamics and Control Group.

Dr. Nijmeijer has been an IFAC Fellow since 2019. He was a recipient of the 2015 IEEE Control Systems Technology Award and a member of the Mexican Academy of Sciences. He is the Graduate Program Director of the TU/e Automotive Systems Program. He is an Editor of *Communications in Nonlinear Science and Numerical Simulations*. He was awarded in 1990 the IEE Heaviside premium. He is appointed honorary knight of the "golden feedback loop" (NTNU, Trondheim, Norway) in 2011. He was an IFAC Council Member in the period 2011–2017. Per January 2015, he is the Scientific Director of the Dutch Institute of Systems and Control (DISC).

Maurice Heemels (Fellow, IEEE) received the M.Sc. (mathematics) and Ph.D. (EE, control theory) degrees *(summa cum laude)* from the Eindhoven University of Technology, Eindhoven, The Netherlands, in 1995 and 1999, respectively.

Currently, he is a Full Professor at ME, TU/e. He held visiting professor positions at ETH, Zürich, Switzerland, in 2001, UCSB, Santa Barbara, CA, USA, in 2008, and the University of Lorraine, Nancy, France, in 2020.

Dr. Heemels was a recipient of the 2019 IEEE L-CSS Outstanding Paper Award and was elected for the IEEE-CSS Board of Governors from 2021 to 2023. He is the Chair of the IFAC Technical Committee on Networked Systems.

Ruud Beerens received the M.Sc. and Ph.D. degrees in mechanical engineering from the Dynamics and Control Group, Eindhoven University of Technology, Eindhoven, The Netherlands, in 2015 and 2020, respectively.

Since 2020, he has been a Mechatronic Development Engineer in the high-tech semiconductor industry. His current research interest includes nonlinear and hybrid control design for high-performance mechatronic systems.

Nathan van de Wouw (Fellow, IEEE) received the Ph.D. degree in mechanical engineering from the Eindhoven University of Technology, Eindhoven, The Netherlands, in 1999.

He is currently a Full Professor at the Mechanical Engineering Department, Eindhoven University of Technology. He is also an Adjunct Full Professor at the University of Minnesota, Minneapolis, MN, USA. He held a (part-time) full professor position at the Delft University of Technology, Delft, The Netherlands, from 2015 to 2019.

Dr. van de Wouw received the IEEE Control Systems Technology Award "for the development and application of variable-gain control techniques for high-performance motion systems" in 2015.